AD NUMBER

AD825758

LIMITATION CHANGES

TO:

Approved for public release; distribution is unlimited.

FROM:

**Distribution authorized to U.S. Gov't. agencies and their contractors;
Administrative/Operational Use; DEC 1967. Other requests shall be referred to National Aeronautics and Space Administration, Goddard Space Flight Center, Greenbelt, MD.**

AUTHORITY

AEDC, USAF ltr, 4 Apr 1973

AEDC-TR-67-273

cy.

TEST OF THE INTELSAT III COMMUNICATION SPACECRAFT AND APOGEE MOTOR UNDER THE COMBINED EFFECTS OF SIMULATED ALTITUDE AND ROTATIONAL SPIN

L. R. Bahor and R. M. Brooksbank
ARO, Inc.

December 1967

ROCKET TEST FACILITY
ARNOLD ENGINEERING DEVELOPMENT CENTER
AIR FORCE SYSTEMS COMMAND
ARNOLD AIR FORCE STATION, TENNESSEE

NOTICES

When U. S. Government drawings specifications, or other data are used for any purpose other than a definitely related Government procurement operation, the Government thereby incurs no responsibility nor any obligation whatsoever, and the fact that the Government may have formulated, furnished, or in any way supplied the said drawings, specifications, or other data, is not to be regarded by implication or otherwise, or in any manner licensing the holder or any other person or corporation, or conveying any rights or permission to manufacture, use, or sell any patented invention that may in any way be related thereto.

Qualified users may obtain copies of this report from the Defense Documentation Center.

References to named commercial products in this report are not to be considered in any sense as an endorsement of the product by the United States Air Force or the Government.

TEST OF THE INTELSAT III COMMUNICATION SPACECRAFT AND APOGEE MOTOR UNDER THE COMBINED EFFECTS OF SIMULATED ALTITUDE AND ROTATIONAL SPIN

L. R. Bahor and R. M. Brooksbank
ARO, Inc.

AF - AEDC
Arnold AFS Tenn

FOREWORD

The test program reported herein was sponsored by the National Aeronautics and Space Administration (NASA) for the Communications Satellite Corporation (COMSAT) under Program Area 921E. Test direction was accomplished by TRW Systems, Inc., with technical assistance from Aerojet-General Corporation (AGC). This test was the result of contractual requirements between COMSAT and their prime contractor, TRW Systems, Inc.

The results of the test were obtained by ARO, Inc. (a subsidiary of Sverdrup & Parcel and Associates, Inc.), contract operator of the Arnold Engineering Development Center (AEDC), Air Force Systems Command (AFSC), Arnold Air Force Station, Tennessee, under contract AF 40(600)-1200. The test was conducted in Propulsion Engine Test Cell (T-3) of the Rocket Test Facility (RTF) on September 8, 1967, under ARO Project No. RC1735, and the manuscript was submitted for publication on November 20, 1967.

Information in this report is embargoed under the Department of State International Traffic in Arms Regulations. This report may be released to foreign governments by departments or agencies of the U. S. Government subject to approval of National Aeronautics and Space Administration, Goddard Space Flight Center, or higher authority. Private individuals or firms require a Department of State export license.

This technical report has been reviewed and is approved.

Edward C. Westwood	Leonard T. Glaser
Captain, USAF	Colonel, USAF
Acting AF Representative, RTF	Director of Test
Directorate of Test	

ABSTRACT

An Aerojet-General Corporation SVM-2 solid-propellant apogee rocket motor installed in an Engineering Model (EM-2) of the INTELSAT III communications spacecraft was fired while spinning at 100 rpm at a pressure altitude of 125, 000 ft. The primary objective of the program was verification of vacuum performance of the apogee motor after being conditioned at 75 ± 5°F. Secondary objectives were to evaluate the thermal and mechanical interactions on the spacecraft as a result of the motor firing. Electrical heaters were utilized in the EM-2 to simulate the heat loads of the active electrical equipment contained in the actual spacecraft. Altitude ignition characteristics and ballistic performance are presented and discussed. Temperature-time histories of thermocouples placed at selected locations on the motor are presented. Spacecraft vibration data and motor exhaust plume heat flux data are also presented and discussed.

CONTENTS

APPENDIXES

I. ILLUSTRATIONS

Figure

Page

II. TABLES

NOMENCLATURE

A_e	Nozzle exit area, $in.^2$
A_t	Nozzle throat area, $in.^2$
C_F	Average thrust coefficient, based on action time, $\frac{I_{vac(action)}}{A_{t(avg)} \int_{t_a} P_{ch} dt}$
F	Motor axial thrust, lb_f
I_{sp}	Specific impulse based on the manufacturer's stated propellant weight and total burn time, lb_f-sec/lb_m
$I_{vac(action)}$	Vacuum impulse based on action time (Fig. 9), lb_f-sec
$I_{vac(total)}$	Vacuum impulse based on total burn time (Fig. 9), lb_f-sec
P_{cell}	Test cell pressure, psia
P_{ch}	Motor chamber pressure, psia
t_0	Zero time, time at which firing voltage is applied to the igniter circuit, sec
t_a	Action time, time interval between 10 percent of maximum chamber pressure during ignition and 10 percent of maximum chamber pressure during tailoff, sec
t_ℓ	Ignition lag time, time interval from zero time to time of increase in chamber pressure, sec
t_t	Total burn time, interval from time of increase in chamber pressure during ignition until the ratio of chamber pressure-to-cell pressure has decreased to a value of 1.3 at tailoff, sec
W	Manufacturer's stated propellant weight, lb_m

SECTION I
INTRODUCTION

The Aerojet-General Corporation (AGC) SVM-2 solid-propellant apogee rocket motor is utilized to propel the Intelsat III communications satellite, designed and constructed by TRW Systems, Inc., into an operating orbit at synchronous altitude from the apogee of the transfer orbit achieved by the long Tank Thor Delta Launch Vehicle (Fig. 1, Appendix I) (Ref. 1).

As part of the TRW Intelsat development program, the motor was installed in a test satellite containing simulated electrical components and fired under the combined effects of rotational spin and simulated altitude. The test satellite is an Engineering Model (EM-2) with a general arrangement as shown in Fig. 2 (Ref. 1) (less the mechanically despun antenna and transmit diplexer). The EM-2 spacecraft utilizes simulated electronic equipment with heater units installed to reproduce the temperatures resulting from operating the actual electronic components. In addition, the hydrazine propellant tanks for the axial and radial thrusters were filled with water to simulate the heat sinks and mass distribution within the actual spacecraft.

The general objectives of this test program were to establish and measure thermal conditions of selected satellite equipment during and after exposure to the effects of the static firing of the SVM-2 solid-propellant motor in a simulated altitude environment and to establish ballistic performance of the SVM-2 solid-propellant motor in a simulated altitude environment while spinning about the longitudinal axis at 100 rpm after the assembly was exposed to a controlled temperature environment of 75 ± 5°F.

Altitude ignition characteristics and ballistic performance of the motor are presented. Motor and spacecraft temperatures and vibration data are discussed.

SECTION II
APPARATUS

2.1 TEST ARTICLE

The AGC SVM-2 solid-propellant rocket motor (Fig. 3) is an apogee motor having the following nominal characteristics:

Length, in.	35
Diameter, in.	23.68
Loaded Weight, lb_m	358
Propellant Weight, lb_m	312
Vacuum Total Impulse, lb_f-sec	82,000
Maximum Chamber Pressure, psia	436
Burn Time, sec	22
Throat Area, $in.^2$	5.96
Nozzle Area Ratio, A/A*	28:1

The chamber assembly is a glass-filament-wound pressure vessel that includes two aluminum bosses for igniter and nozzle installation and an integral skirt incorporating an aluminum thrust ring. The chamber assembly is internally insulated with a molded silica-filled V-45 Buna-N® rubber material. Basic dimensions and materials of the chamber are shown in Fig. 3 (Ref. 1).

The pressure vessel consists of two longitudinal and four circumferential layers of Owens-Corning S-994 glass roving, preimpregnated with 58-68 Shell resin system. The longitudinal layers are wound over the insulator which includes integral igniter and nozzle bosses. The aluminum thrust ring is attached to the chamber with type 341 glass cloth which is held in position by circumferential layers of roving.

The grain assembly is a case-bonded, thermally cured, polybutadiene propellant grain. The propellant, designated ANB-3066, is case-bonded to the insulation with SD-851-2 rubber copolymer. The configuration of the propellant grain consists of eight fins in the forward head section and a cylindrical bore which provide the required burning surface.

A partially submerged contoured nozzle with a 28:1 area ratio has been selected for this motor. The complete nozzle assembly has six major components: entrance cap, throat insert, throat backup, nozzle housing, nozzle housing insulator, and exit cone. A weather seal of polyurethane foam is attached to the exit cone.

The entrance cap consists of a composite wrap of laminates of carbon-cloth-reinforced phenolic resin.

The throat insert is silver-infiltrated tungsten to provide minimum erosion. The insert is retained by a throat backup, also made of compression-molded phenolic resin with carbon cloth reinforcement.

The nozzle housing is machined from 6061-T6 aluminum and is attached to the chamber by an integral flange. The submerged portion

of the nozzle housing is insulated with General Tire and Rubber V-44 molded rubber. The exit-cone liner, made of parallel wrapped layers of silica-phenolic resin tape, is bonded to the housing and overwrapped with a 0.030-in. layer of adhesive-impregnated glass cloth.

The KR 80000-09 safe-and-arm device, which is also the first element of the ignition train, contains two independent squibs (US Flare ES-003), which can be activated either singularly or simultaneously. The squib is rated at 1 amp no-fire and is qualified for all-fire at 4.3 amp. The safe-and-arm device is hermetically sealed and filled with 98 percent dry nitrogen and 2 percent helium to ensure consistent performance under extreme environmental conditions.

The igniter is a controlled-pressure igniter which utilizes boron-potassium-nitrate (BPN) pellets (AGC 32087, Types II and III) as pyrotechnics. The primary interface between the safe-and-arm device and the igniter is identical with the successful Minuteman ignition system. This design feature was selected to retain the proved performance reproducibility of the Minuteman primary ignition train.

The one-piece main igniter housing is a molded-epoxy fiber glass chamber with multiple nozzles, which direct the igniter flame to the propellant surfaces. The chamber is lined with a molded Styrofoam® cup to hold and cushion the main charge pellets.

The primary charge consists of 8 gm of AGC 32087 Type II pellets. The main charge assembly contains 136 gm of AGC 32087 Type III pellets which are packed between the annulus of the chamber wall and the flame tube.

The igniter chamber is held in place by a conventional steel retaining ring. The safe-and-arm device is sealed by a face seal O-ring between the safe-and-arm flange and the chamber adapter.

2.2 INSTALLATION

The motor spacecraft assembly was cantilever mounted from the aft bearing of a spin fixture assembly in Propulsion Engine Test Cell (T-3) (Ref. 2). The spin assembly was mounted on a thrust cradle, which was supported from the cradle support stand by three vertical and two horizontal double-flexure columns (Fig. 4). The spin fixture assembly consisted of a 10-hp squirrel-cage-type drive motor, a drive shaft and thrust pylon, and an aft bearing assembly. The spin fixture rotates counterclockwise, looking upstream. Electrical leads to and from the

igniter, pressure transducers, thermocouples, and accelerometers on the rotating motor were provided through a 170-channel slip-ring assembly mounted on the drive shaft. Axial thrust was transmitted through the drive shaft-thrust bearing assembly to two load cells mounted just forward of the thrust bearing.

Pre-ignition pressure altitude was maintained in the test cell by a steam ejector operating in series with the RTF exhaust gas compressors. During motor firing, the motor exhaust gases were used as the driving gas for the 35.5-in.-diam ejector-diffuser system to maintain test cell pressure at an acceptable level.

2.3 INSTRUMENTATION

Instrumentation was provided to measure axial thrust; test cell and motor chamber pressures; nozzle, motor case, and spacecraft temperatures; motor and spacecraft vibration levels; motor exhaust plume heat flux; and motor-spacecraft rotational speed. Table I (Appendix II) presents instrumentation ranges, recording methods, and system accuracies for all reported parameters.

The axial thrust measuring system consisted of two double-bridge, strain-gage-type load cells mounted in the axial double-flexure column forward of the thrust bearing on the rocket motor centerline.

Unbonded strain-gage-type transducers were used to measure test cell pressure. Bonded strain-gage-type transducers were used to measure motor chamber pressure. Chromel®-Alumel® (CA) thermocouples were bonded to the motor case and nozzle (Fig. 5), and iron-constantan (IC) thermocouples were bonded to the spacecraft (Fig. 6) to measure temperatures before, during, and after motor firing. Piezoelectric-type accelerometers were used to measure the dynamic effects of the apogee motor on the spacecraft. Thermocouple and accelerometer locations are presented in Figs. 5 and 6. Rotational speed of the motor and spin rig assembly was determined from the output of a magnetic pickup.

Radiometers and calorimeters were used to measure the rocket motor exhaust radiation heat flux. Narrow-angle (7.5-deg) radiometers equipped with a sapphire (0.3- to 6-μ transmission band) window were mounted on the diffuser duct perpendicular to the motor centerline. This position resulted in the radiometers being approximately 2 in. downstream of the nozzle exit plane of the rocket motor (Fig. 6b). The heating rate calorimeters (black sensing disk) were located on and

perpendicular to the aft surface of the spacecraft (Fig. 6b). The radiometers and calorimeters were designed to measure the temperature gradient between the center and the periphery of the active sensor area. This temperature gradient is directly proportional to the heating rate. Therefore, the millivolt output is a direct determination of the heating rate provided that:

1. The temperature of the heat sink does not change, and
2. The emissivity of the sensor disk remains constant.

The data presented in this report utilized calibration curves of heat flux (Btu/ft^2-sec) as a function of millivolt output (supplied by TRW, Inc.), and no additional corrections were made.

The output signal of each measuring device was recorded on independent instrumentation channels. Primary data were obtained from four axial-thrust channels, four test cell pressure channels, and three motor chamber pressure channels. These data together with those obtained from the two radiometers and two calorimeters were recorded as follows: Each instrument output signal was indicated in totalized digital form on a visual readout of a millivolt-to-frequency converter. A magnetic tape system, recording in frequency form, stored the signal from the converter for reduction at a later time by an electronic digital computer. The computer provided a tabulation of average absolute values for each 0.10-sec time increment and total integrals over the cumulative time increments.

The output signal from the magnetic rotational speed pickup was recorded in the following manner: A frequency-to-analog converter was triggered by the pulse output from the magnetic pickup and in turn supplied a square wave of constant amplitude to the electronic counter and oscillograph recorders. The scan sequence of the electronic counter was adjusted so that it displayed directly the motor spin rate in revolutions per minute.

The millivolt outputs of the thermocouples were recorded on magmetic tape from an analog-to-digital converter at a sampling rate for each thermocouple of 50 samples/sec during the motor firing and for 5 sec during each 2-min interval for a total of 1 hr after the firing. The millivolt outputs of the accelerometers were conditioned through individual charge amplifiers prior to transmission through slip rings. The amplified outputs were recorded on FM analog magnetic tape and played back to a photographically recording, galvanometer-type oscillograph at a later time.

A recording oscillograph was used to provide an independent back-up of all operating instrumentation channels except the temperature, calorimeter, radiometer, and accelerometer systems. Selected channels of thrust and pressures were recorded on null-balance, potentiometer-type strip charts for analysis immediately after a motor firing. Visual observation of the firing was provided by a closed-circuit television monitor. High-speed, motion-picture cameras provided a permanent visual record of the firings.

2.4 CALIBRATION

The thrust calibration weights, thrust load cells, pressure transducers, and accelerometers were laboratory calibrated prior to usage in this test. After installation of the measuring devices in the test cell, thrust load cells were again calibrated at sea-level, nonspin ambient conditions and at simulated altitude while spinning at 100 rpm.

The pressure recording systems were calibrated by an electrical, four-step calibration, using resistances in the transducer circuits to simulate selected pressure levels. The axial thrust instrumentation systems were calibrated by applying to the thrust cradle known forces, which were produced by deadweights acting through a bell crank. The calibrator is hydraulically actuated and remotely operated from the control room. Thermocouple and accelerometer recording instruments were calibrated by using known millivolt levels to simulate thermocouple and accelerometer outputs. The calibration curves for the narrow-angle radiometers and calorimeters were supplied by TRW, Inc.

After the motor firing, with the test cell still at simulated altitude pressure, the recording systems were recalibrated to determine any shift.

SECTION III
PROCEDURE

The AGC SVM-2 solid-propellant rocket motor arrived at AEDC on August 28, 1967. The motor was visually inspected for possible shipping damage and radiographically inspected for grain cracks, voids, or separations. During storage in an area temperature conditioned at 75 ± 5°F, the motor and spacecraft were checked to ensure correct fit of mating hardware, and the electrical resistance of the igniter was

measured. The nozzle throat and exit diameters were measured, the entire motor assembly was weighed and photographed, and the thermocouples and accelerometers were installed. The chamber pressure instrumentation and squib assembly were installed, and a pressure leak test was conducted on the motor. Motor and spacecraft surfaces were mated and aligned. The nozzle plug was removed to accomplish the pre-fire inspection and leak test, then replaced, and punctured for the firing.

After installation of the motor-spacecraft assembly in the test cell, the spacecraft centerline was axially aligned with the spin axis within ±0.010 in. by rotating the motor-spacecraft assembly and measuring the deflection of nozzle interior and nozzle exit plane surfaces with a dial indicator. Instrumentation connections were made, and a nozzle exit closure was installed on the rocket motor. A continuity check of all electrical systems was performed. A balance check was performed by rotating the motor-spacecraft assembly at a speed of 100 rpm.

Pre-fire, sea-level calibrations were completed, the test cell pressure was reduced to the desired pressure altitude condition, and spinning of the unit was started. After spinning had stabilized at 100 rpm, a complete set of altitude calibrations was taken. The various heaters, which simulate the thermal loads of the active electronic components within the actual spacecraft, were activated to produce the desired temperatures at various locations within the spacecraft.

Once the temperature had stabilized, the final operation prior to firing the motor was to adjust the firing circuit to provide the desired 4.5-amp current to each of two igniter squibs. The entire instrumentation measuring-recording complex was activated, and the motor was fired while spinning (under power) at 100 rpm. The igniter safe-and-arm device was electrically actuated to the "arm" position prior to test cell evacuation. This operation was performed through electrical connections which bypassed the slip-ring assembly. Actual motor ignition, however, was accomplished through electrical connections passing through the slip-ring assembly.

Spinning of the motor was continued for approximately 60 min after burnout, during which time post-fire calibrations were accomplished. The unit was decelerated slowly until rotation had stopped, and another set of calibrations was taken. The test cell pressure was then returned to ambient conditions, and the motor and spacecraft were inspected, photographed, and removed to the storage area. Post-fire inspections at the storage area consisted of measuring the throat and exit diameters of the nozzle, weighing the motor, and photographically recording the post-fire condition of the motor and spacecraft.

SECTION IV
RESULTS AND DISCUSSION

A test program was conducted in Propulsion Engine Test Cell (T-3) utilizing an Engineering Model (EM-2) of the Intelsat III spacecraft containing an Aerojet-General Corporation SVM-2 solid-propellant rocket motor. The motor was fired at a pressure altitude of 125,000 ft with the spacecraft-motor assembly spinning about the longitudinal axis at 100 rpm. The spacecraft and motor were conditioned to 75 ± 5°F prior to the establishment of the desired test cell pressure. Once altitude conditions were attained, the internal heaters within the spacecraft were activated, and power was regulated to simulate the thermal output of the active electrical devices which are contained in the actual Intelsat III Spacecraft.

The primary objective of the test program was verification of the vacuum ballistic performance and structural integrity of the Aerojet-General Corporation (AGC) SVM-2 solid-propellant apogee rocket motor. Secondary objectives were to determine the thermal and dynamic interactions between the motor and the spacecraft. The resulting data are presented in both tabular and graphical form. Altitude ignition characteristics and ballistic performance of the motor are presented. Motor and spacecraft temperatures, motor exhaust plume heat flux, and system structural integrity are discussed. Vibration data from the motor and spacecraft are also discussed.

Motor performance data are summarized in Table II, and a summary of motor physical dimensions is presented in Table III. The average measured total impulse was corrected to vacuum conditions by the methods presented in Section 4.2. Specific impulse values are presented using both the manufacturer's stated propellant weight and the motor expended mass determined from AEDC pre- and post-fire motor weight. When more than one instrumentation channel of equal accuracy was used to obtain values of a single parameter, the average value is discussed and used to calculate the data presented.

4.1 ALTITUDE IGNITION CHARACTERISTICS

The motor was successfully ignited at a simulated altitude of 125,000 ft. The motor pre-fire temperature was 79°F. An analog trace of thrust, chamber pressure, and cell pressure during motor ignition is presented in Fig. 7.

Ignition lag time, defined as the time interval between application of current to the igniter squibs and the first perceptible rise in chamber pressure was 0.007 sec. The peak chamber pressure during ignition was 380 psia.

4.2 BALLISTIC PERFORMANCE

The variations of thrust, chamber pressure, and test cell pressure during the motor firing are shown in Fig. 8. The maximum vacuum thrust and maximum chamber pressure obtained during the test were 5028 lb_f and 460 psia, respectively, and occurred 4.80 sec after ignition.

Since the exhaust nozzle does not operate fully expanded at the low chamber pressure encountered during tailoff, the measured thrust data cannot be corrected to vacuum conditions by adding the product of cell pressure integral and nozzle exit area; therefore, total and action times were segmented, and the method used to determine vacuum impulse is illustrated in Fig. 9. The exhaust nozzle flow breakdown was considered to have occurred simultaneously with the exhaust diffuser flow breakdown (as indicated by a rapid increase in cell pressure). The flow at the nozzle throat was considered sonic until the chamber-to-cell pressure ratio had decreased to a value of 1.3. The motor tailoff characteristics are presented in Fig. 10. Chamber pressure decayed smoothly during the entire tailoff event.

The total burn time (t_t), defined as the interval from the first indication of chamber pressure at ignition until the chamber-to-cell pressure ratio had decreased to 1.3, was 71.80 sec (Fig. 10). Action time (t_a), defined as the time interval between 10 percent of maximum chamber pressure during ignition and 10 percent of maximum chamber pressure during tailoff, was 25.40 sec.

Vacuum-corrected total impulse, based on total burn time, was 88,719 lb_f-sec. The vacuum correction was 0.39 percent of the measured impulse (accumulated from ignition until nozzle flow breakdown). Vacuum specific impulse based on vacuum total impulse and the manufacturer's stated propellant weight was 284.35 lb_f-sec/lb_m. Vacuum specific impulse based on vacuum total impulse and pre- and post-fire weight difference was 281.05 lb_f-sec/lb_m. Vacuum specific impulse based on vacuum action impulse and pre- and post-fire weight difference was 279.35 lb_f-sec/lb_m. Vacuum thrust coefficient based on action time and the average of pre- and post-fire nozzle throat area was 1.846.

4.3 MOTOR CASE AND SPACECRAFT TEMPERATURES

Thermocouples were bonded to the motor case and spacecraft (Figs. 5 and 6) to measure temperatures during the motor firing and the 60-min period after the firing. Temperature-time histories from selected thermocouples on the motor and spacecraft are presented in Fig. 11.

The maximum temperatures and the time of occurrence at selected locations are summarized below:

Location	Temperature, °F	Time after Ignition
Nozzle Exit Cone (TM11)	651 (Fig. 11c)	170 sec
Nozzle Attachment Flange (TM8)	467 (Fig. 11b)	17 min
Motor Case Wall (Cylindrical) (TM5)	467 (Fig. 11a)	7 min
Motor Case Wall (Forward Section) (TM4A)	478 (Fig. 11a)	7 min
Solar Panel (T34)	137 (Fig. 11j)	29 sec
Motor Support Housing (T14)	180 (Fig. 11d)	25 min
Nozzle Close-Out Ring (T36)	311 (Fig. 11i)	40 sec
Thermal Insulator (T10)	386 (Fig. 11e)	4.5 min
Spacecraft Electrical Components (T17)	142 (Fig. 11g)	65 min

Six electrical heaters were installed inside selected components shown in Fig. 6 in order to reproduce the temperatures resulting from operating the actual electronic components. Once the desired component pre-fire temperatures were reached, the output of the electrical heaters was maintained at constant levels throughout both the firing and the thermal soak-back period (60 min). Six thermocouples (T20 through T25) were bonded to these components to record the temperature increase due to the motor firing. The temperature history for the six components is summarized below:

Component	Desired Pre-Fire Temperature Limits, °F	Actual Pre-Fire Temperature, °F	Maximum Temperature (°F) and Time (min) after Firing
High Level TWT "A"	135 to 146	140	165 at 65
High Level TWT "B"	135 to 146	140	161 at 65
Transponder "A"	92 to 102	99	126 at 65
Transponder "B"	92 to 102	100	125 at 57
Converter	85 to 95	78	106 at 65
Battery	60 to 70	70	96 at 65

As shown, the actual pre-fire temperature was within the desired limits on all components except the converter.

4.4 STRUCTURAL INTEGRITY

Post-fire photographs of the motor case interior, nozzle, and spacecraft are presented in Figs. 12, 13, and 14, respectively. Post-fire inspection of the SVM-2 motor case revealed large areas of insulation-to-case separation (Fig. 12), which exposed small sections of the fiber glass case material. Slight interior discoloration of the fiber glass was evident in the areas of exposure.

Delamination of the nozzle fiber glass overwrap material was evident along the external surface of the exit cone (Fig. 13). Post-fire inspection also revealed areas of separation in the nozzle throat entrance cap material (Fig. 13c) (reinforced carbon-phenolic fabric).

Pre- and post-fire inspection data indicated a decrease in throat area of approximately 3.14 percent during the firing. The decrease in nozzle exit area was approximately 0.60 percent during the firing (exhaust product deposition was not removed prior to throat and exit diameter measurements).

No physical damage to the spacecraft assembly resulted during motor operation. However, physical damage to the Kapton®-covered stainless steel aft end cover was sustained (Fig. 14) as a result of the momentary recirculation of hot rocket exhaust products (blowback) into the test cell when the nozzle and diffuser flow breakdown occurred.

4.5 PLUME HEAT FLUX

Two water-cooled, narrow angle (7.5-deg) radiometers and two calorimeters were used to obtain rocket exhaust plume heat flux data. The radiometers were mounted to the lip of the water-cooled diffuser duct (Fig. 6b), and the calorimeters were secured to the aft section of the spacecraft (Fig. 6b).

The variation of the heat flux data with time is presented in Fig. 15. A maximum radiation heat flux of 12.6 Btu/ft^2-sec was measured by the radiometer and occurred 14.0 sec after ignition. During actual motor operation, radiation heat flux measured by the radiometers was substantially higher than that measured by the calorimeters. This was a result of the radiometer's narrow field of view (7.5 deg) which allowed its sensing element to be focused directly on the exhaust plume. The calorimeters, which incorporated a much larger field of view (≈ 180 deg), were located upstream of the exhaust plume and measured only the average heat flux over a larger effective area.

The sudden increase in heat flux level, recorded by the calorimeters, occurring approximately 23 sec after ignition, is attributed to convective heat transfer caused by the influx of hot exhaust products into the test cell as a result of nozzle and diffuser flow breakdown. The radiometer elements, which were shielded, were largely unaffected by nozzle flow breakdown.

4.6 SHOCK AND VIBRATION DATA

The motor and spacecraft were rigidly secured to the spin-rig which was mounted to a flexure supported thrust cradle as shown in Fig. 4. The accelerometers were located on the motor and spacecraft as shown in Fig. 6. As a result, the vibration data recorded by the accelerometers are composite signals of the vibration of the spacecraft and the vibration of the spin rig-thrust cradle assembly.

Data taken during the ignition transient from accelerometers positioned to record axial acceleration are presented in Fig. 16. The data in Fig. 16 are presented in the form of an analog trace of the accelerometer output. Accelerometer A-5, located on the solar panel of the spacecraft, recorded a maximum peak-to-peak acceleration of 153g's (Fig. 16a). Accelerometer A-3, located on the wobble damper bracket of the spacecraft (Fig. 16b), recorded a maximum acceleration of 49g's. A maximum acceleration of 175g's (Fig. 16c) was recorded by accelerometer A-1 located on the igniter boss. Accelerometer A-4 located on the equipment platform recorded a maximum acceleration of 24g's (Fig. 16d).

The smaller vibration levels shown approximately 0.100 sec after motor ignition (Fig. 16) are representative of the levels during steady-state motor operation.

SECTION V
SUMMARY OF RESULTS

One Aerojet-General Corporation SVM-2 solid-propellant apogee rocket motor was fired at a pressure altitude of 125,000 ft while mounted in an Engineering Model of the Intelsat III communications spacecraft which was spinning at 100 rpm about its longitudinal axis. The spacecraft and motor were conditioned to a temperature of 75 ± 5°F prior to firing the motor. The results are summarized as follows:

1. The time interval between application of current to the igniter squibs and the first perceptible rise in chamber pressure was 0.007 sec.
2. The time interval from the time of increase in chamber pressure during ignition and the time at which the chamber-to-cell pressure ratio reached a value of 1.3 at tailoff (t_t) was 71.8 sec.
3. The time interval beginning when chamber pressure had risen to 10 percent of maximum (excluding ignition peak) and ending when chamber pressure had fallen to 10 percent of maximum at tailoff (t_a) was 25.40 sec.
4. Vacuum total impulse based on t_t was 88,719 lb_f-sec. Vacuum specific impulse, based on the manufacturer's stated propellant weight and t_t, was 284.35 lb_f-sec/lb_m.
5. The average vacuum thrust coefficient, based on t_a and the average of pre- and post-fire nozzle throat areas, was 1.846.
6. The maximum nozzle exit cone temperature was approximately 651°F and occurred 170 sec after motor ignition. The maximum motor case temperature was approximately 478°F and occurred 7 min after motor ignition.
7. The maximum value of motor exhaust plume radiation heat flux measured at the nozzle exit was 12.6 Btu/ft^2-sec and occurred 14.0 sec after motor ignition.
8. The nozzle throat and exit areas decreased 3.14 and 0.60 percent, respectively, as a result of the firing.
9. Post-fire inspection of the rocket motor assembly revealed large areas of insulation-to-case separation which exposed small portions of the fiber glass case material. This was a result of thermal soak-back following motor burnout. Delamination of the fiber glass nozzle overwrap and nozzle throat entrance cap was also observed. The spacecraft assembly did not sustain physical damage during apogee motor operation.

REFERENCES

1. "Test Plan for Intelsat III Spacecraft Apogee Motor Integration Test at the Arnold Engineering Development Center." TRW Systems, Redondo Beach, California, August 11, 1967 (D-00024).
2. Test Facilities Handbook (6th Edition). "Rocket Test Facility, Vol. 2." Arnold Engineering Development Center, November 1966.

APPENDIXES

I. ILLUSTRATIONS

II. TABLES

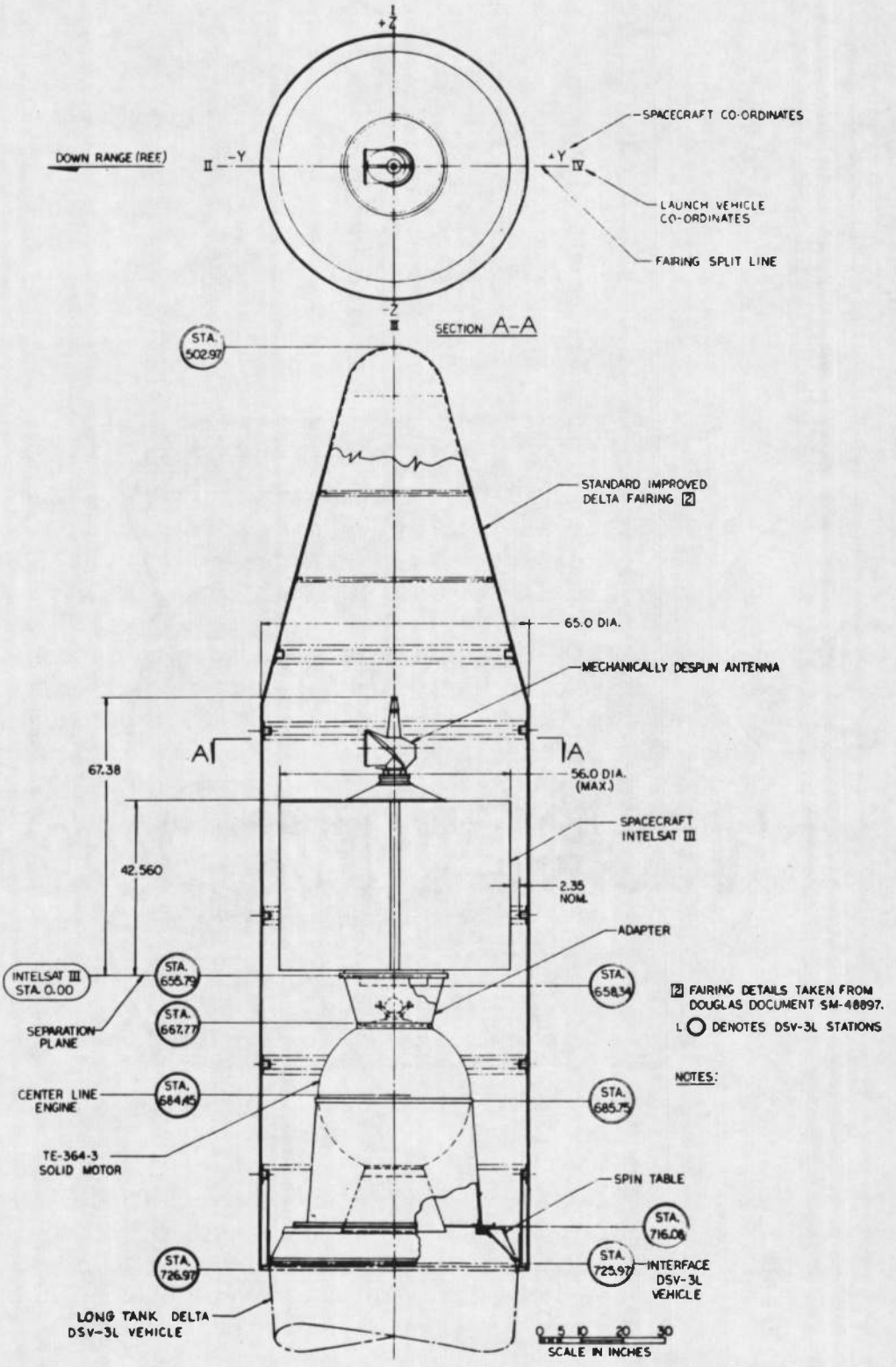

Fig. 1 Schematic of Intelsat III Launch Configuration

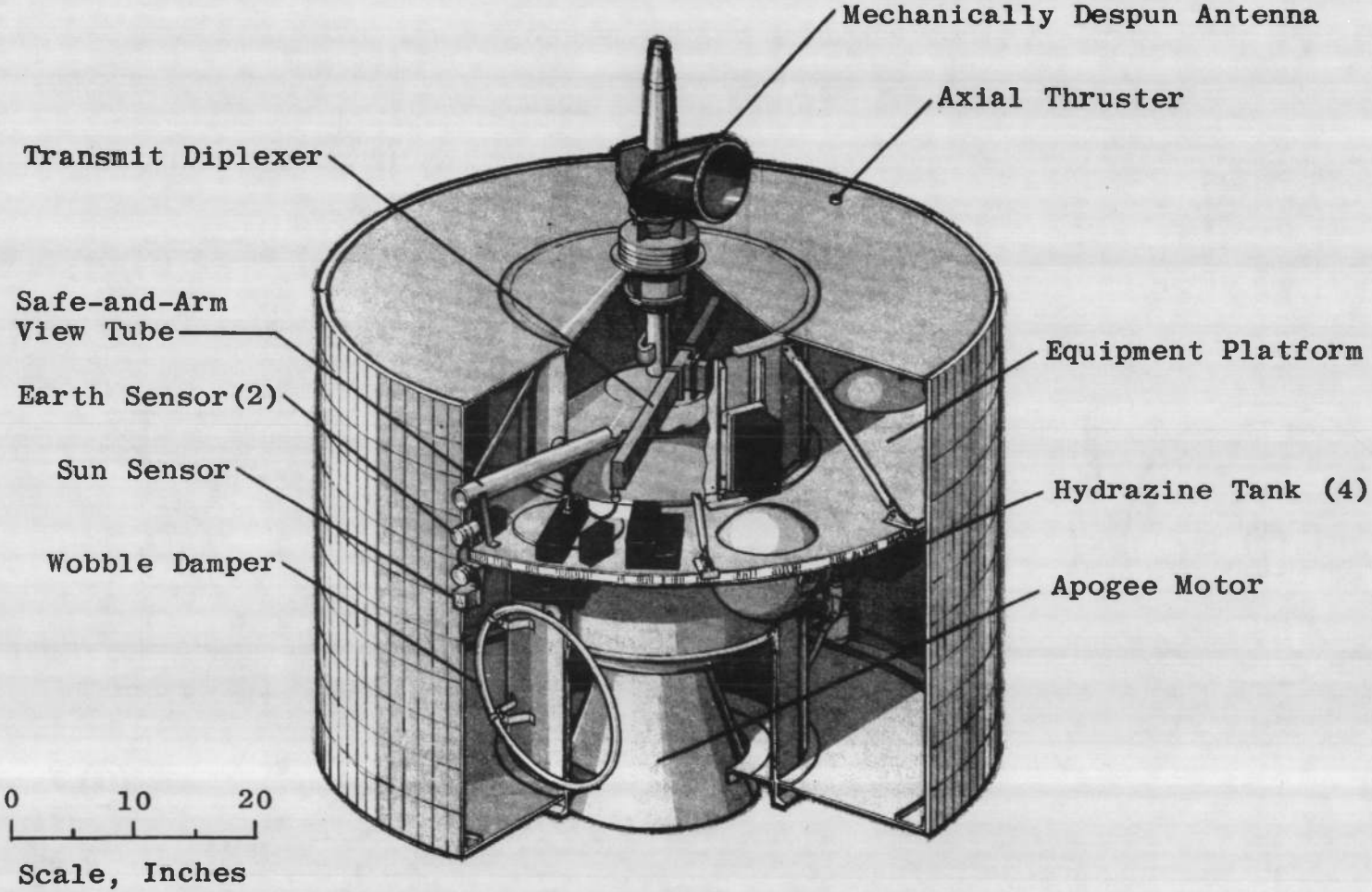

a. Schematic

Fig. 2 Comsat Intelsat III Communications Spacecraft

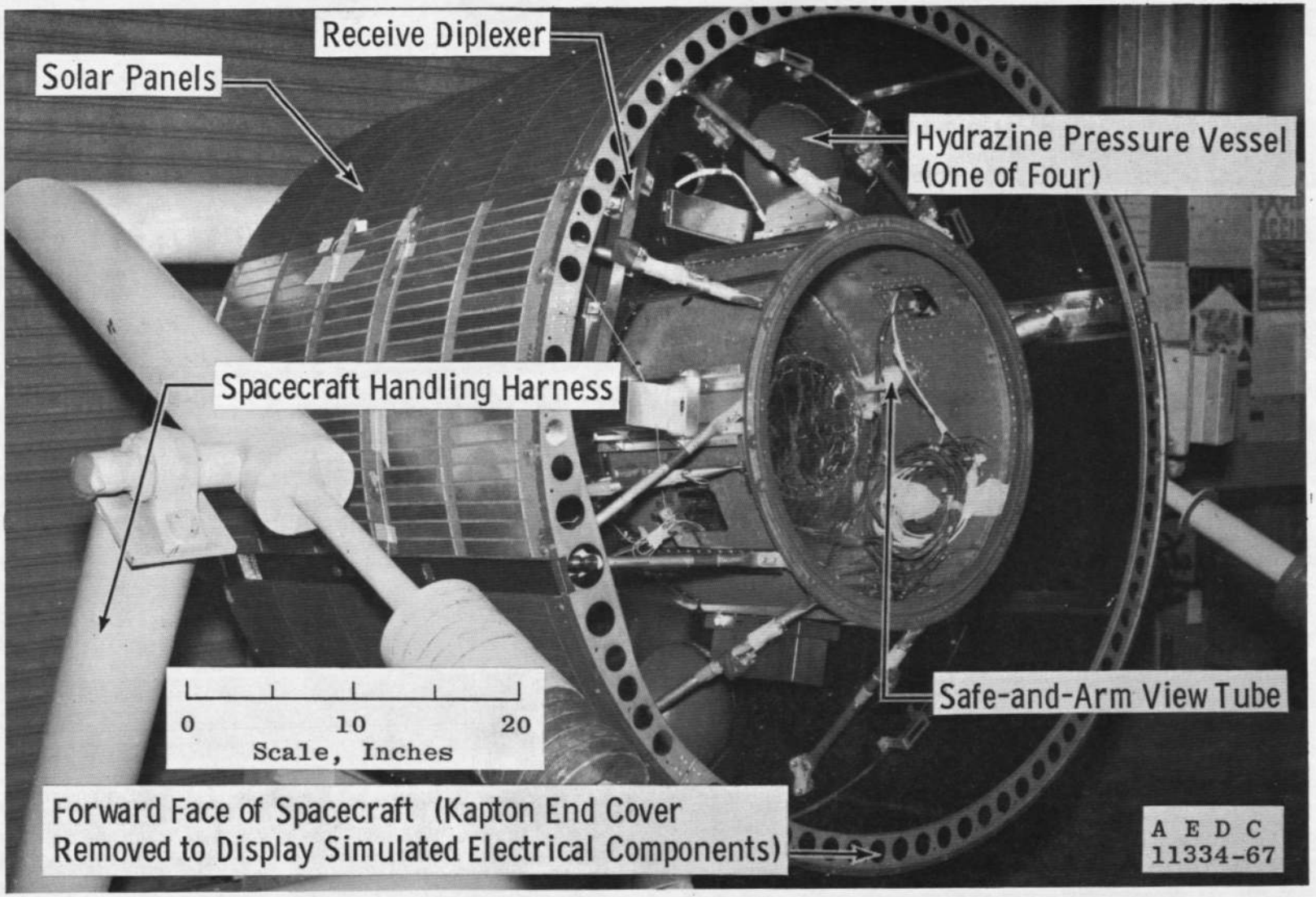

b. Photograph (Forward Section with End Cover Removed)

Fig. 2 Continued

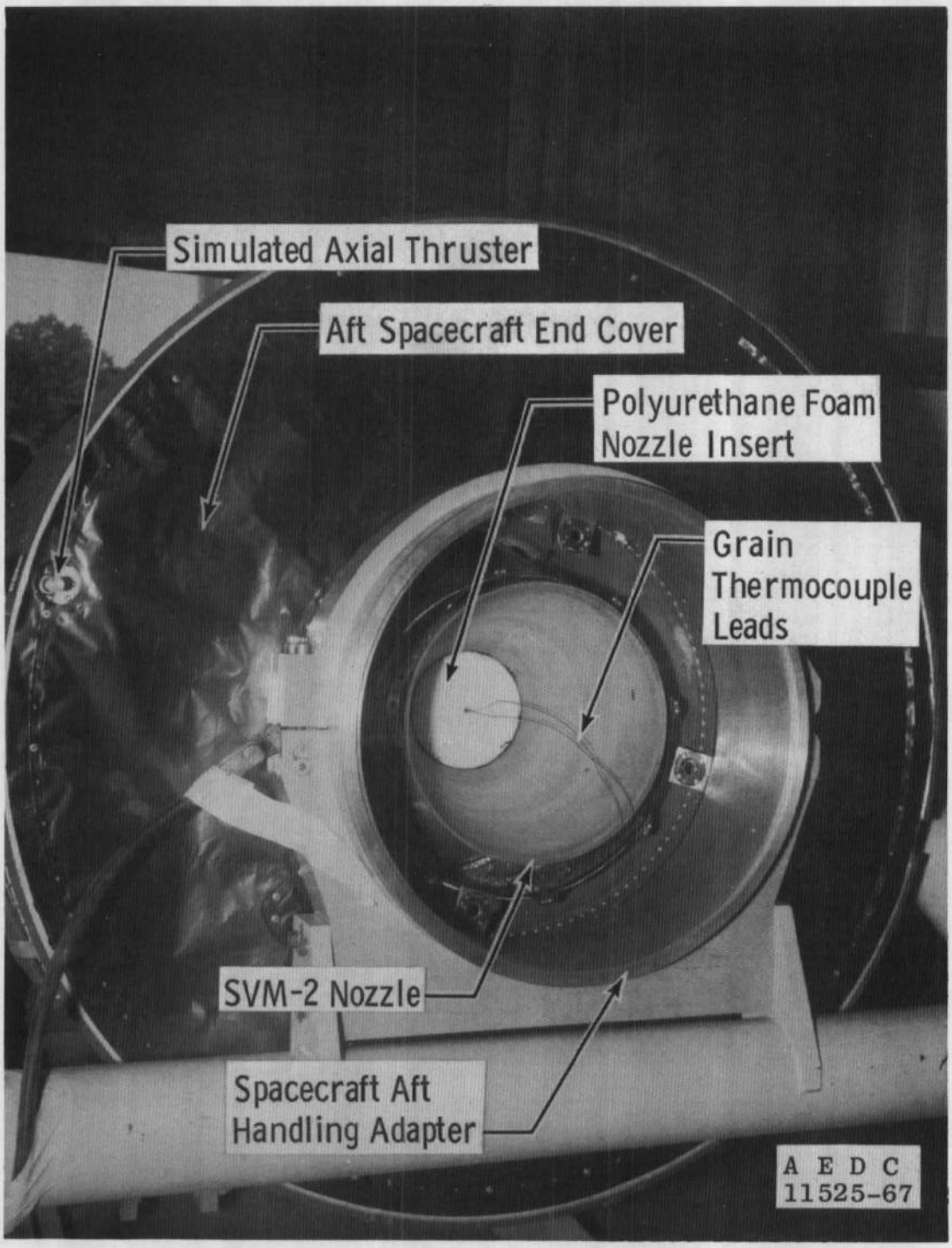

c. Photograph (Aft Section with Apogee Motor Installed)

Fig. 2 Concluded

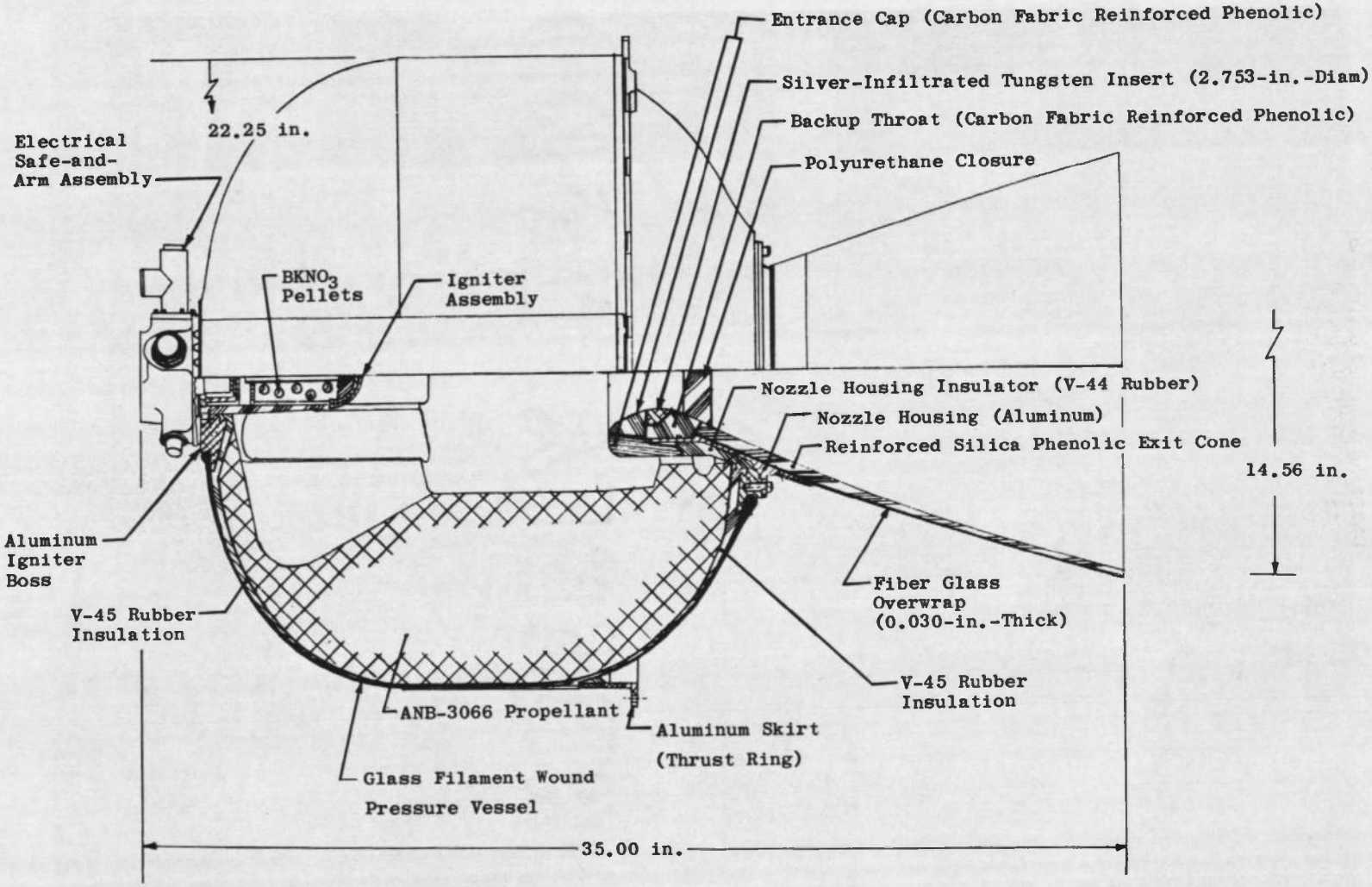

a. Schematic

Fig. 3 Aerojet-General Corporation SVM-2 Apogee Motor

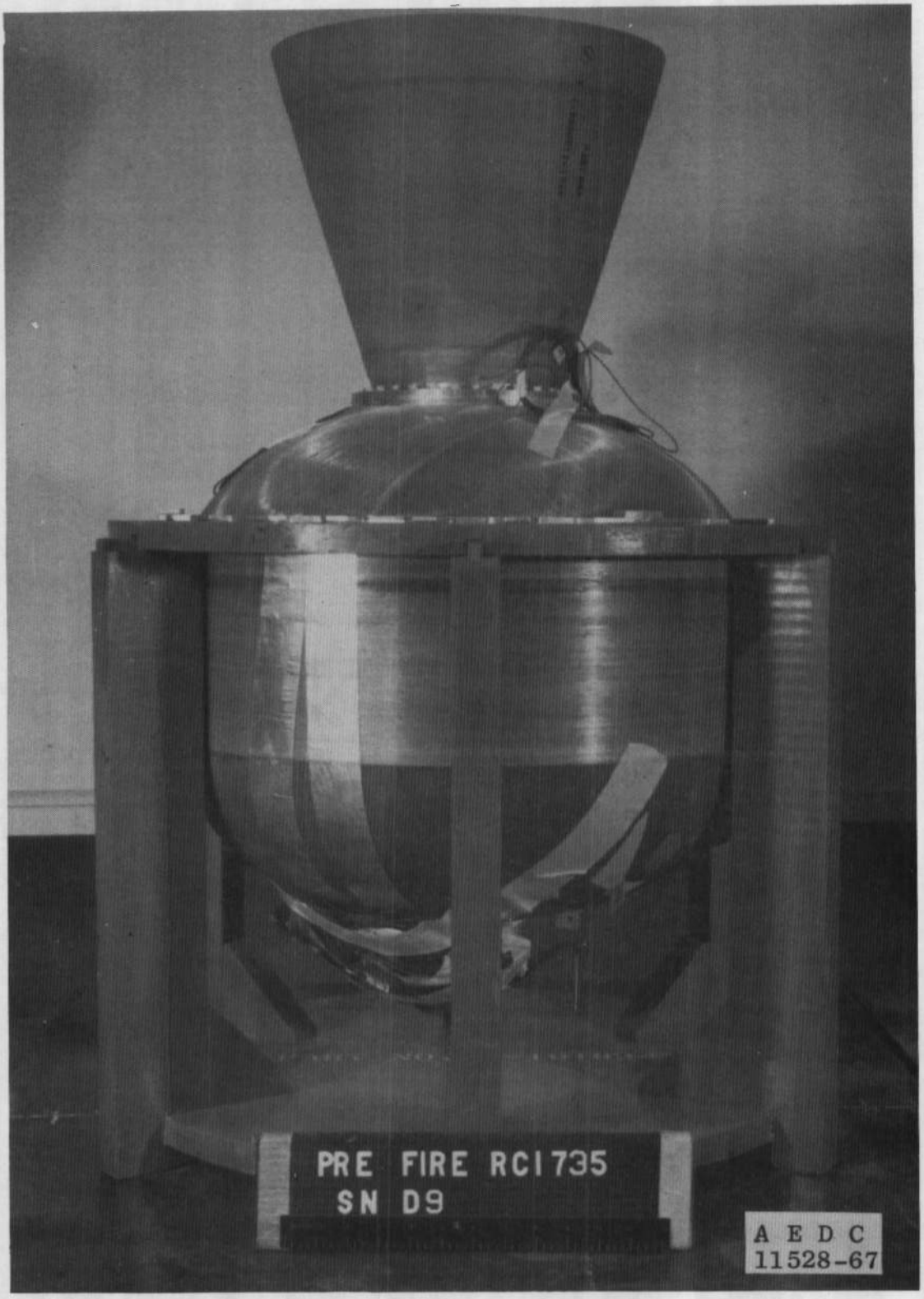

b. Photograph

Fig. 3 Concluded

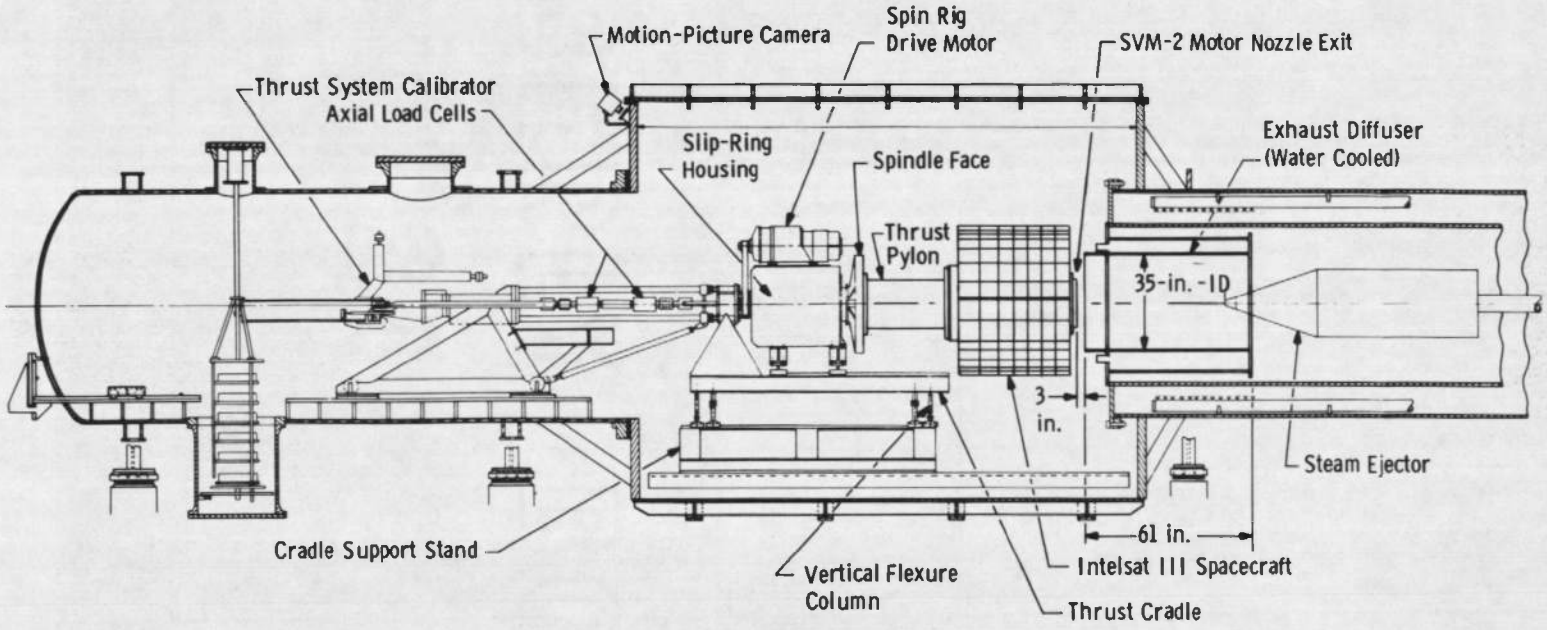

a. Schematic

Fig. 4 Installation of the Intesat III Spacecraft Assembly in the T-3 Test Cell

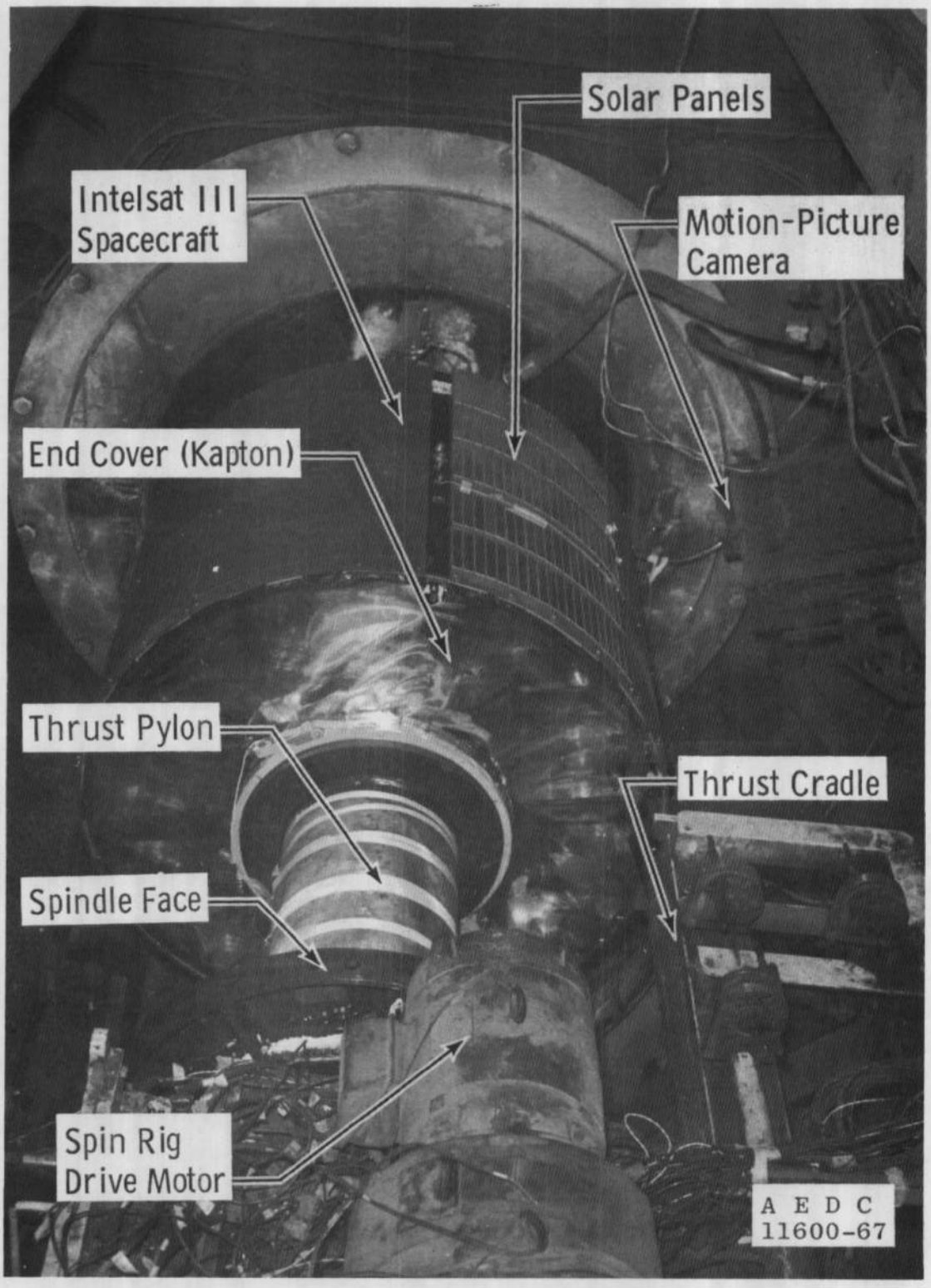

b. Photograph (Overall View)

Fig. 4 Continued

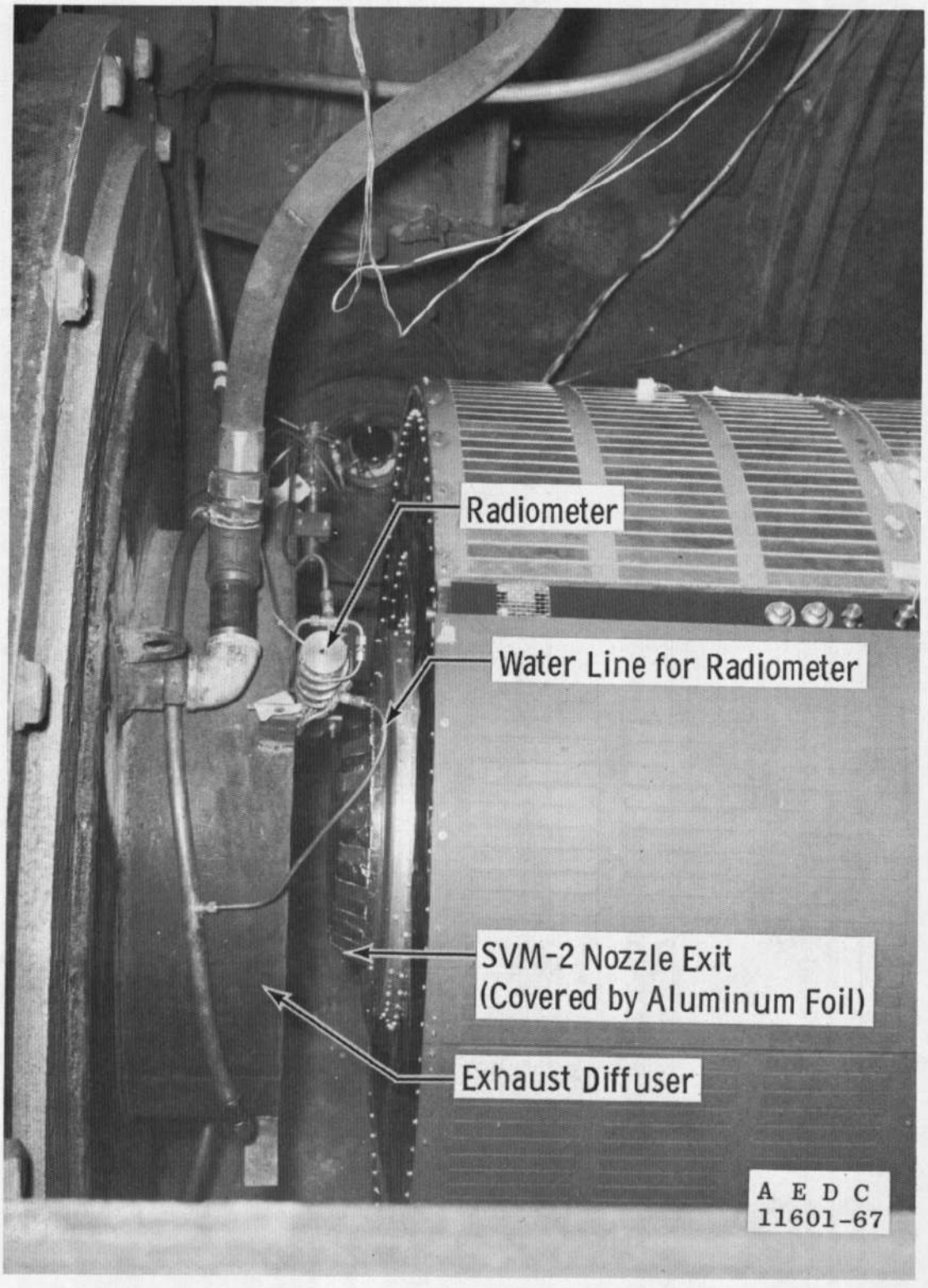

c. Photograph (Overhead View of Spacecraft Aft Surface)

Fig. 4 Concluded

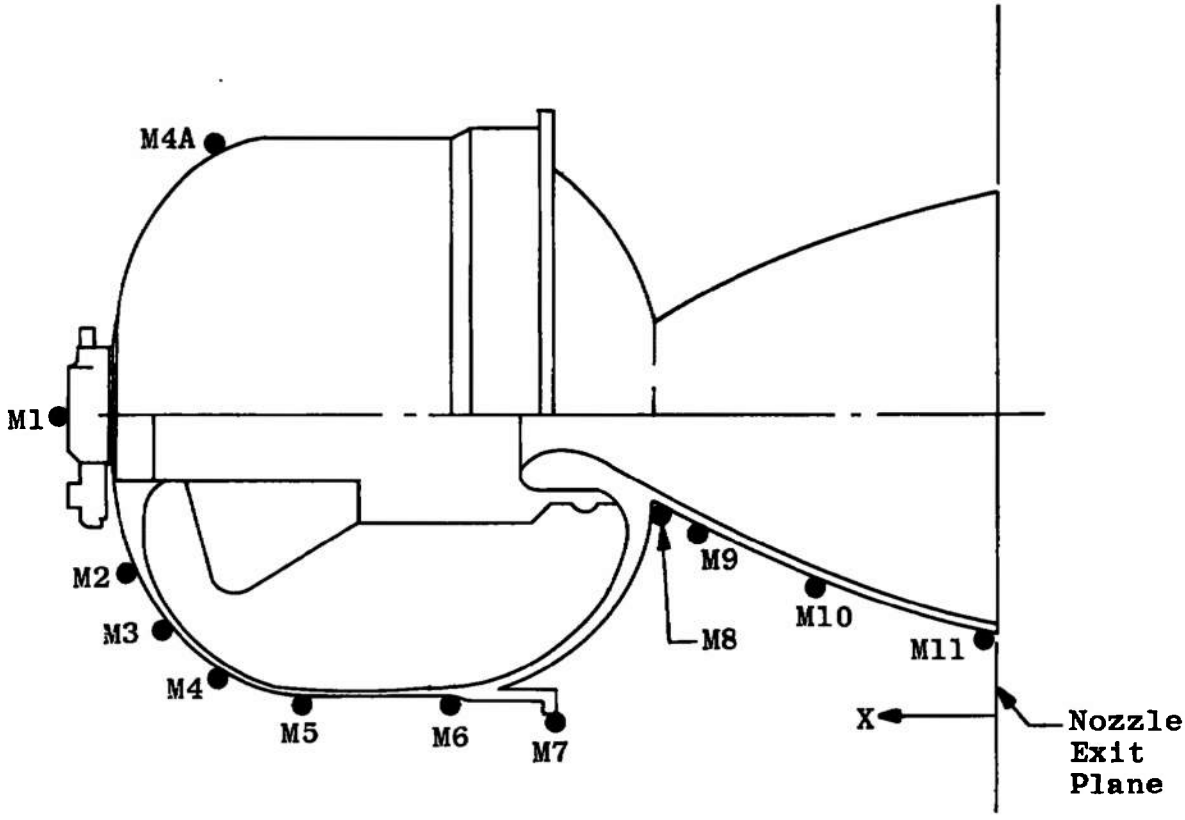

TC No.	X, in.	Angular Location, deg
M1	35.00	0 (On Motor Centerline)
M2	32.40	285
M3	31.80	285
M4	28.90	285 (Propellant Peak)
M4A	28.90	105 (Propellant Peak)
M5	25.60	285
M6	19.40	285
M7	17.50	272 (Skirt)
M8	13.00	285
M9	11.50	285
M10	6.00	285
M11	0.25	285

NOTE: Angular Locations Measured Clockwise (Looking Upstream) from Index Notch on Nozzle Flange

Fig. 5 Motor Thermocouple Location

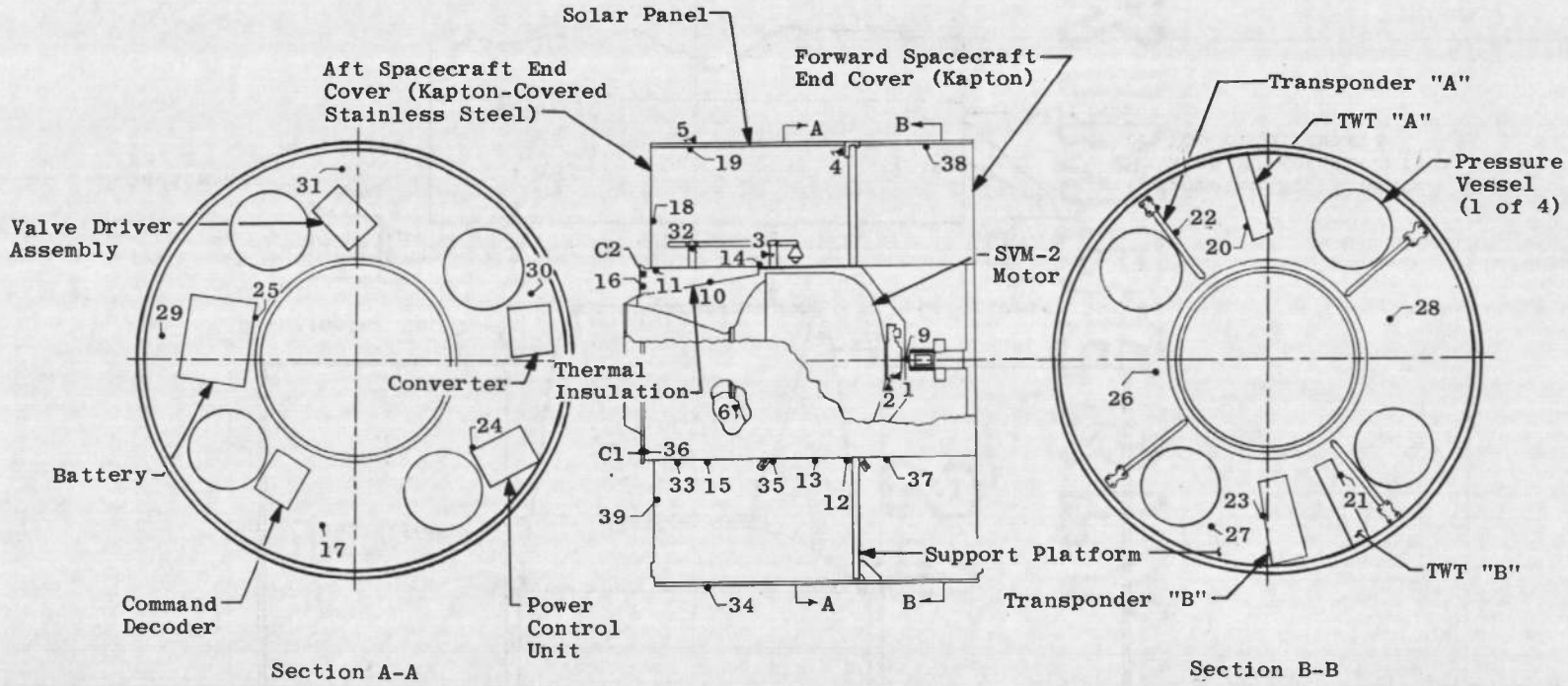

a. Spacecraft Thermacouple, Accelerameter, and Calorimeter Lacations

Fig. 6 Temperature, Heat Flux, and Vibratian Instrumentatian Lacations

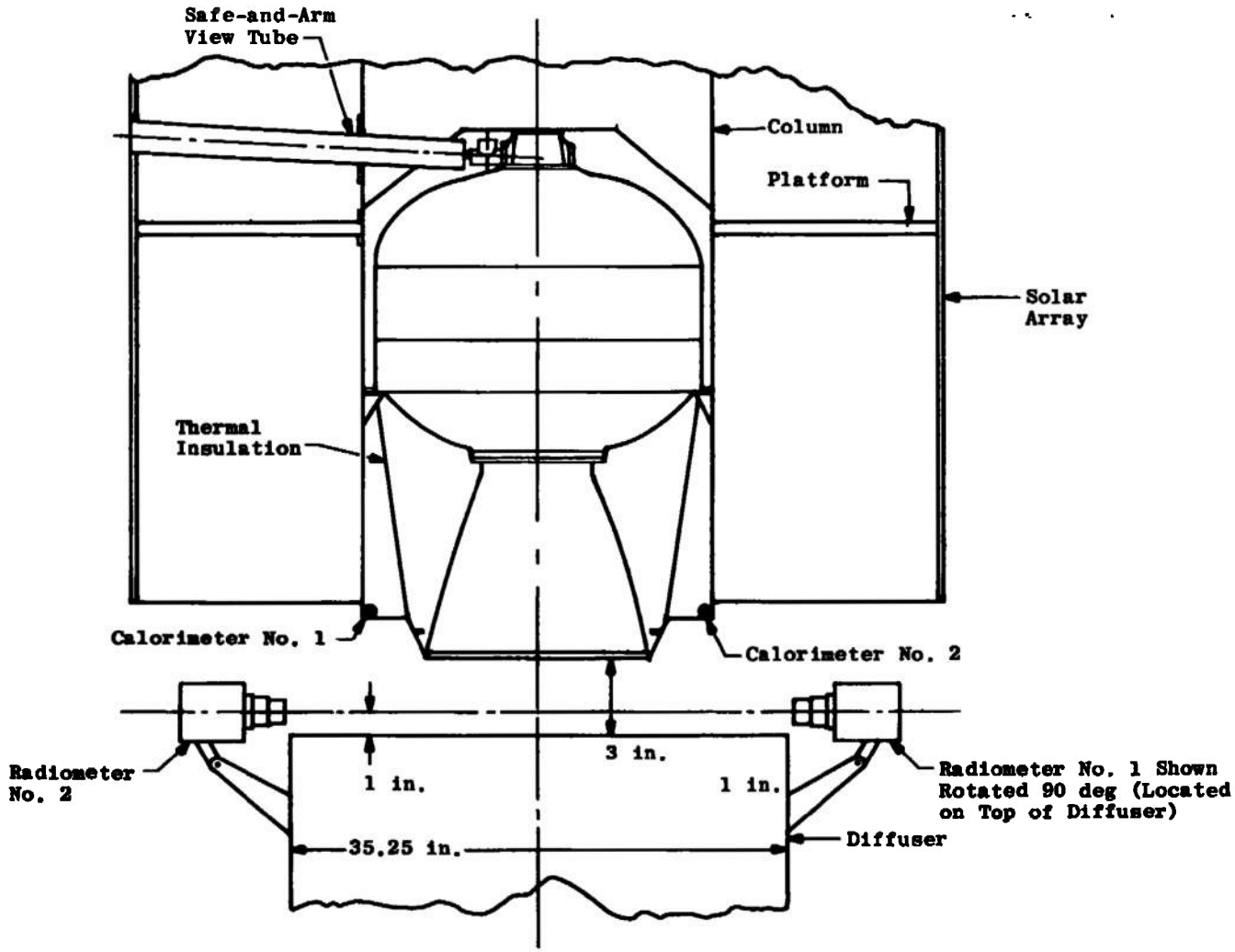

b. Detailed Location of Calorimeters and Radiometers

Fig. 6 Concluded

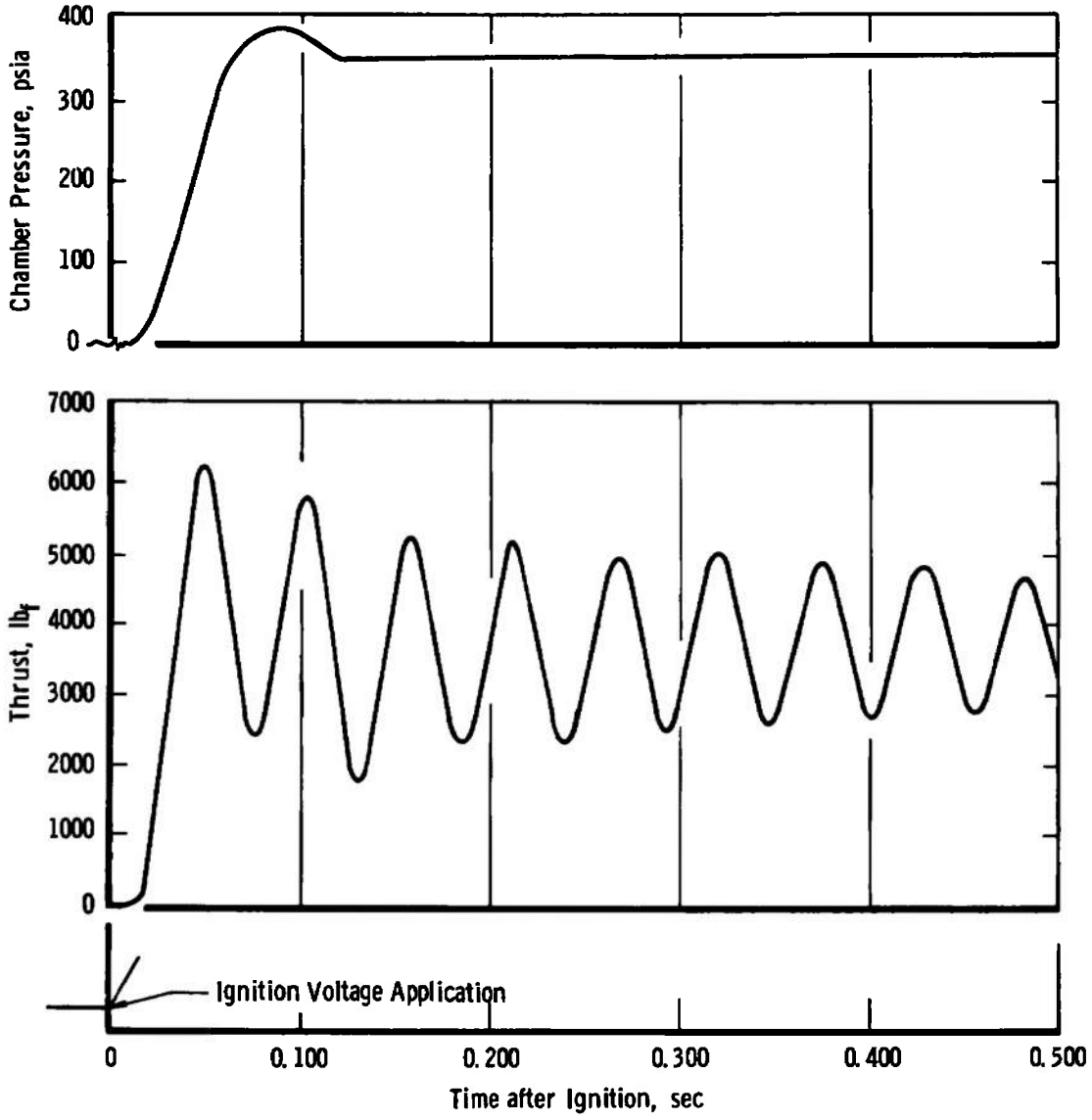

Fig. 7 Analog Trace of the Ignition Event

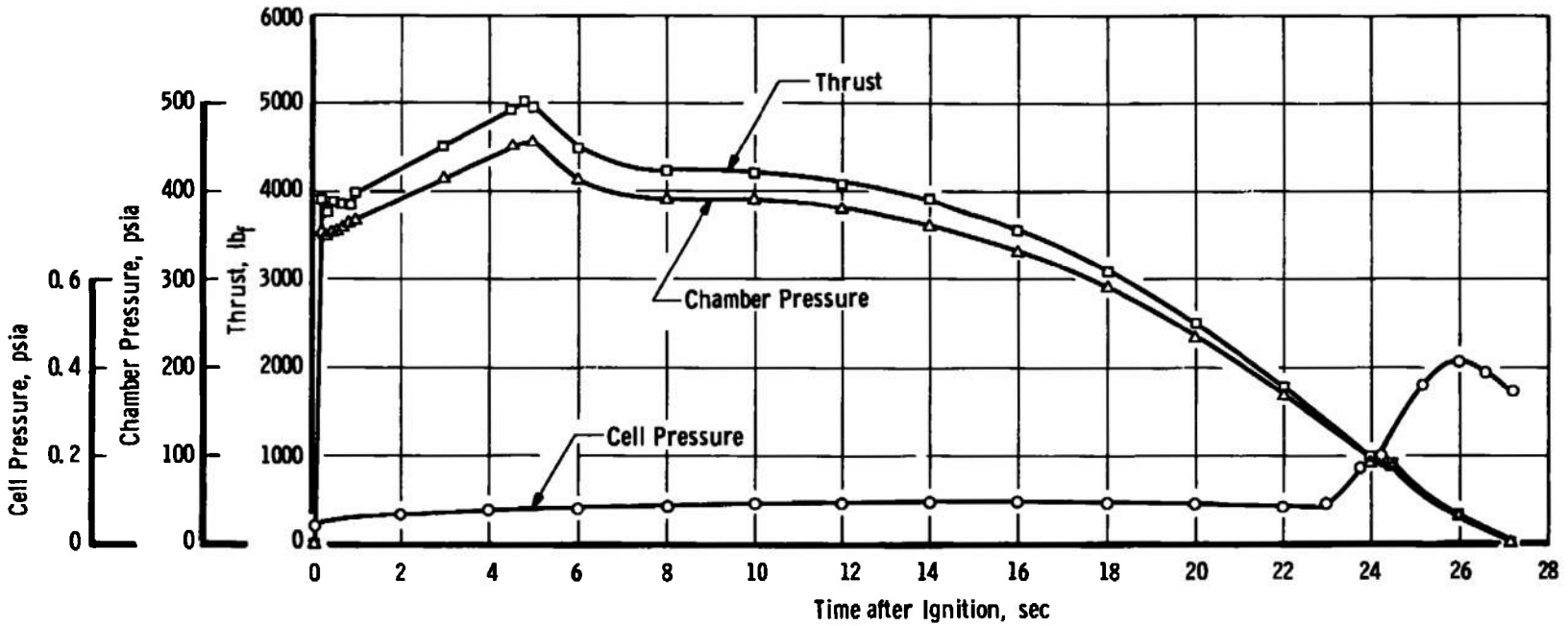

Fig. 8 Variation of Thrust, Chamber Pressure, and Test Cell Pressure during Firing

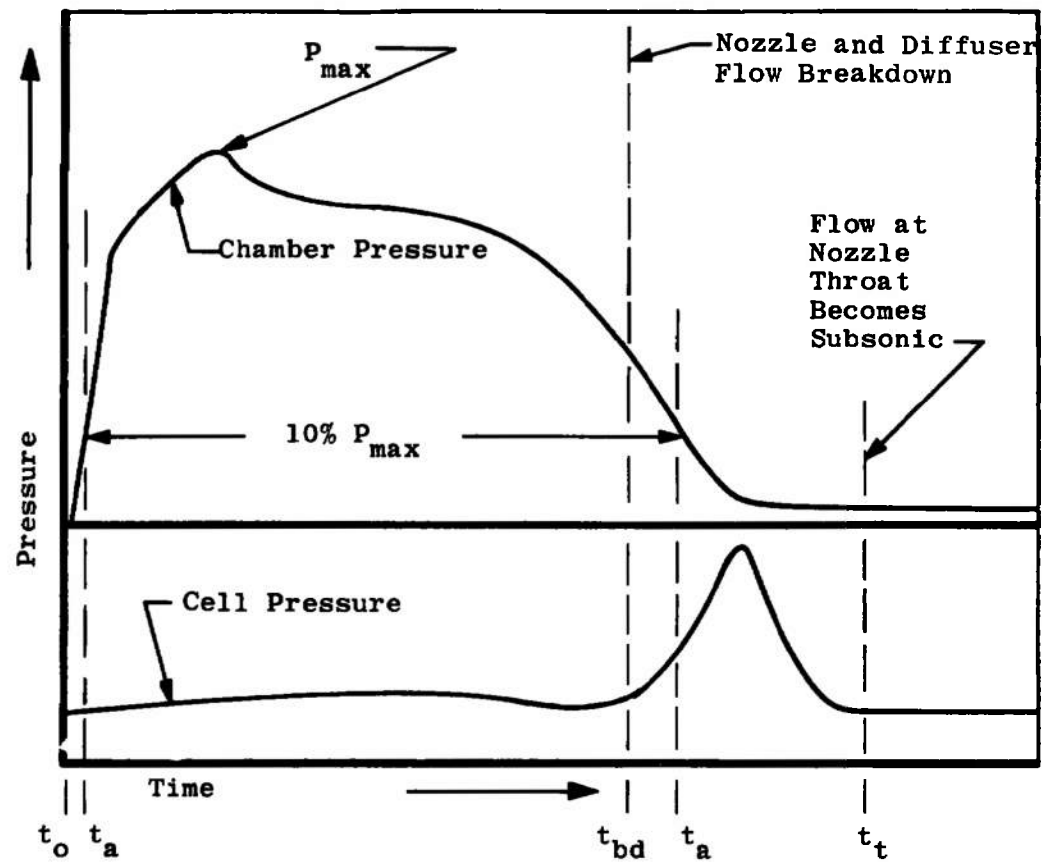

$$I_{vac_{total}} = \int_{t_o}^{t_{bd}} F\,dt + A_{ex_{(avg)}} \int_{t_o}^{t_{bd}} P_{cell}\,dt + \bar{c}_f\, A_{th_{(post)}} \int_{t_{bd}}^{t_t} P_{ch}\,dt$$

$$I_{vac_{action}} = \int_{t_{a_{ignition}}}^{t_{bd}} F\,dt + A_{ex_{(avg)}} \int_{t_a}^{t_{bd}} P_{cell}\,dt + \bar{c}_f\, A_{th_{(post)}} \int_{t_{bd}}^{t_{a_{tailoff}}} P_{ch}\,dt$$

where: $\bar{c}_f = \dfrac{F_{measured} + P_{cell}\, A_{ex_{(post)}}}{P_{ch}\, A_{th_{(post)}}}$ and was established from data during the time interval from 21.60 to 22.60 sec after first indication of chamber pressure.

Fig. 9 Definition of Vacuum Total and Vacuum Action Impulse

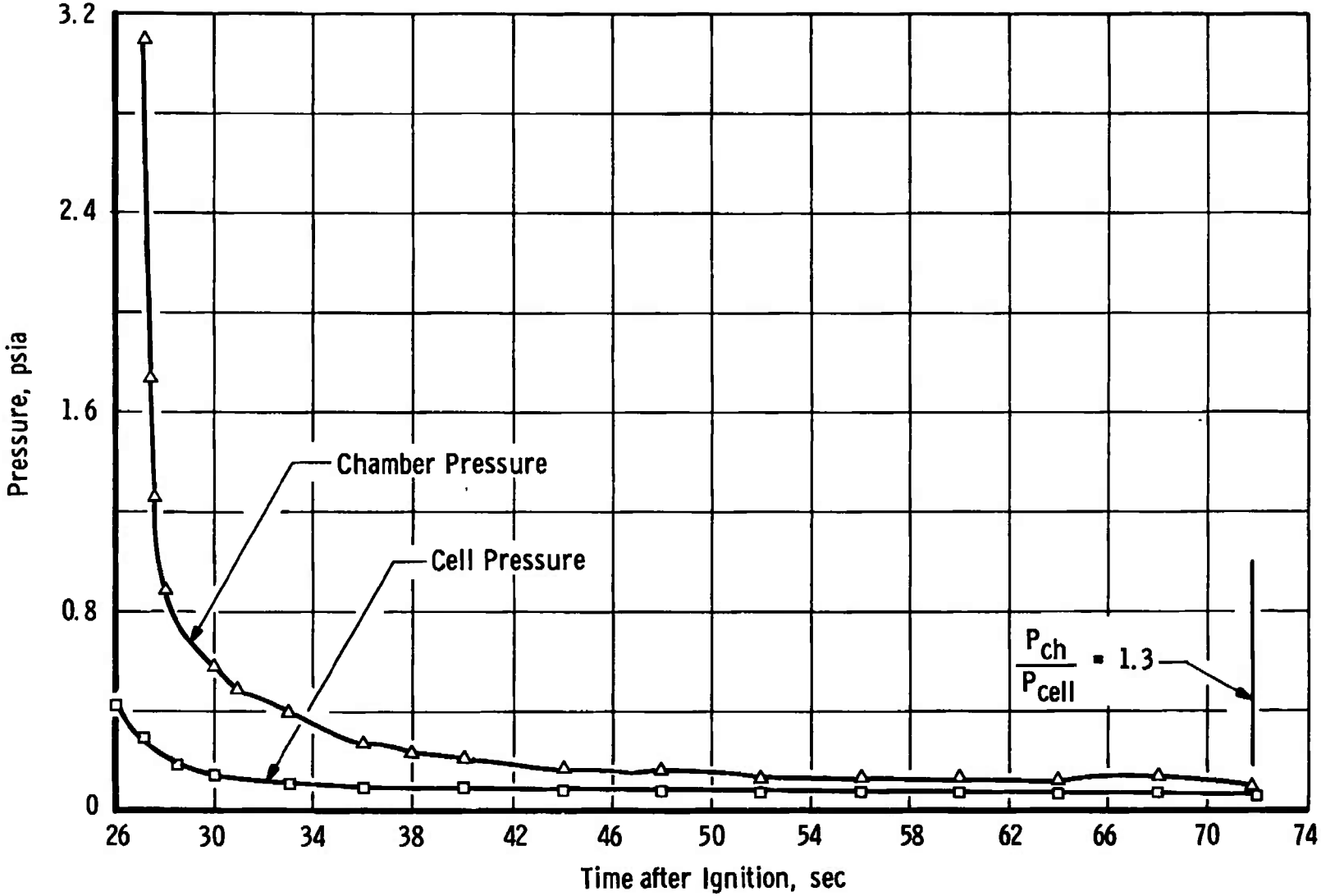

Fig. 10 Motor Tailoff Characteristics (Low-Range Chamber Pressure from 3.1 psia to Chamber Pressure-to-Cell Pressure Ratio of 1.3)

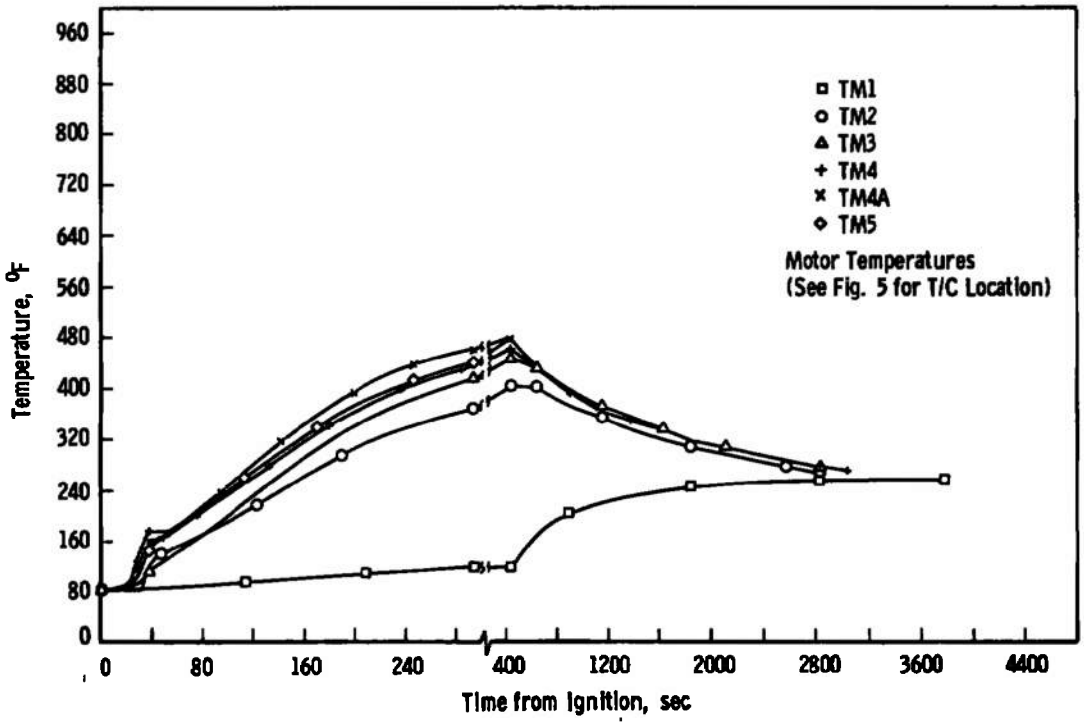

a. TM1, TM2, TM3, TM4, TM4A, and TM5

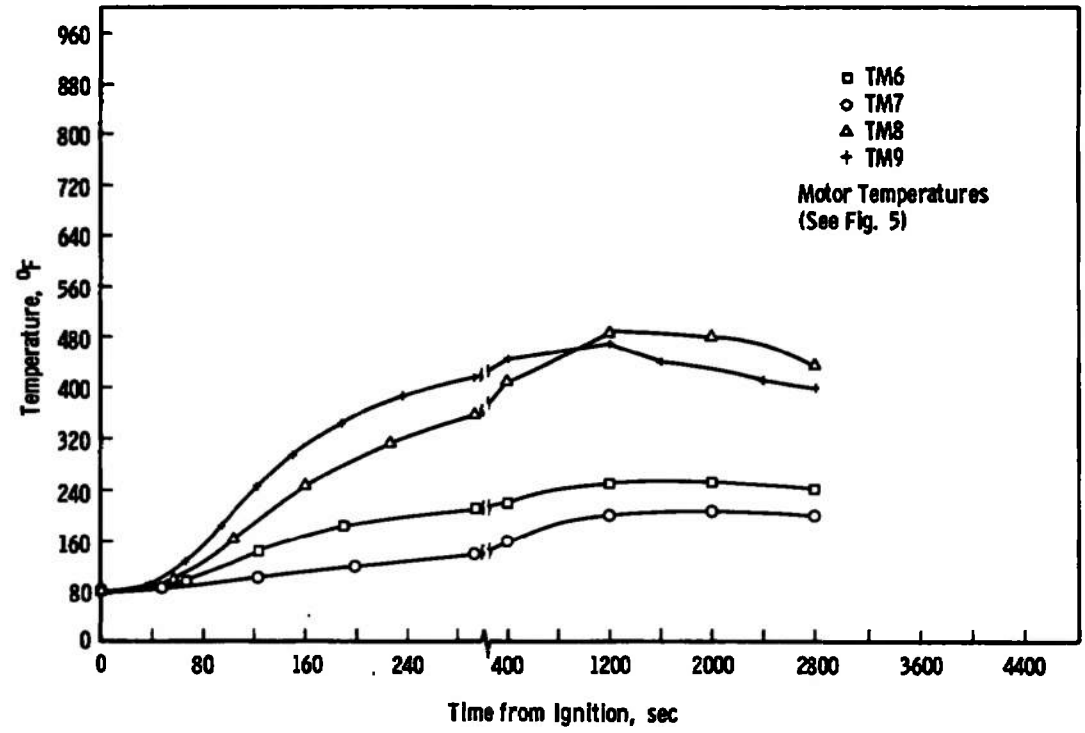

b. TM6, TM7, TM8, and TM9

Fig. 11 Temperature-Time Histories of the Spacecraft and Apogee Motor

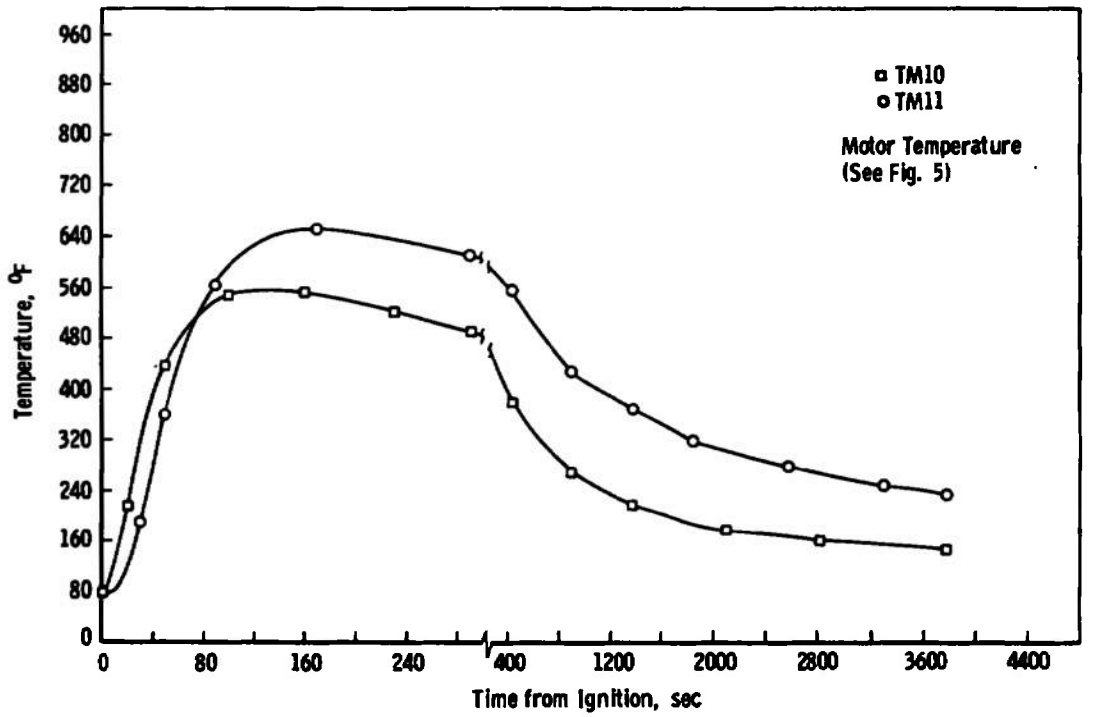

c. TM10 and TM11

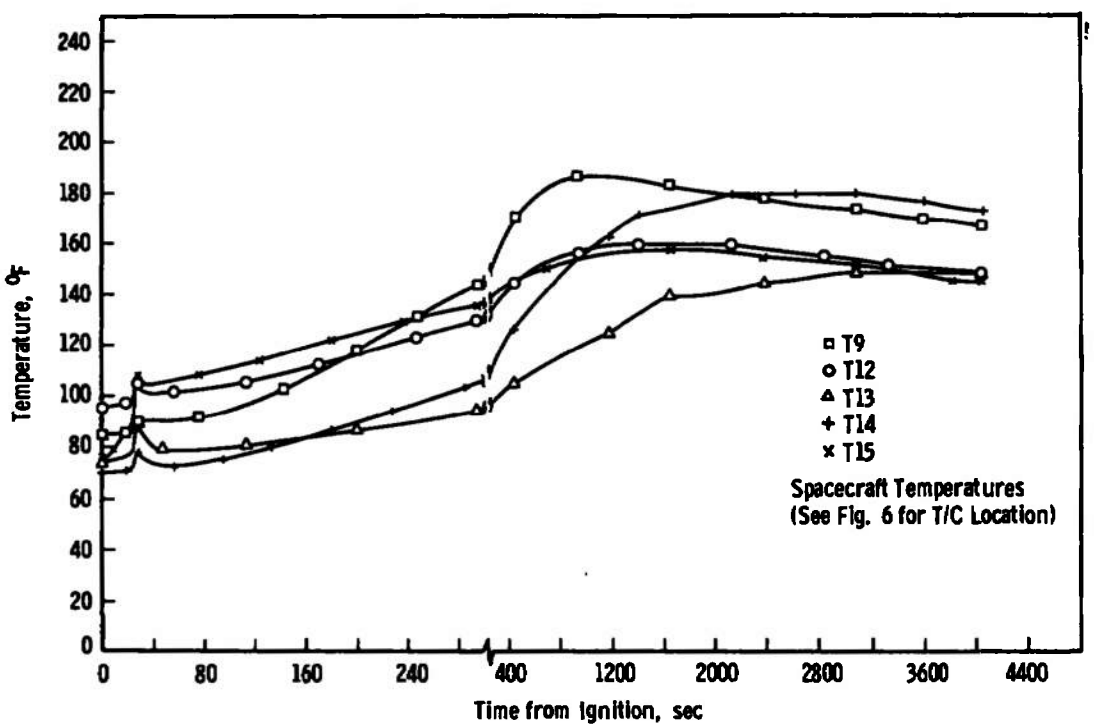

d. T9, T12, T13, T14, and T15

Fig. 11 Continued

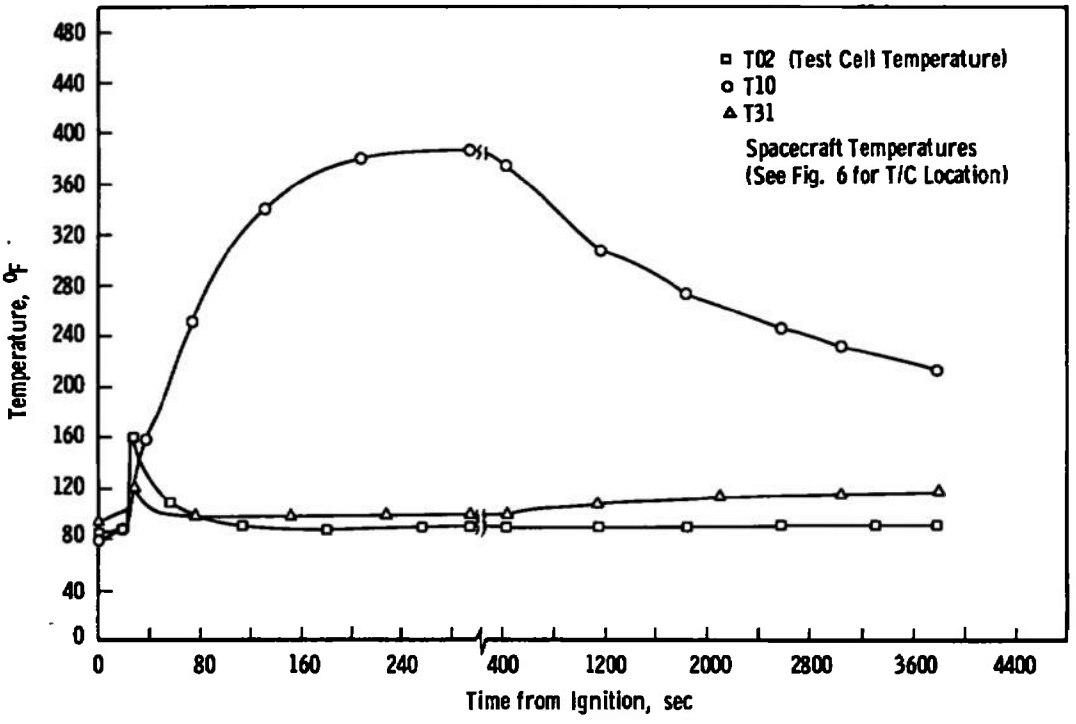

e. T2, T10, and T31

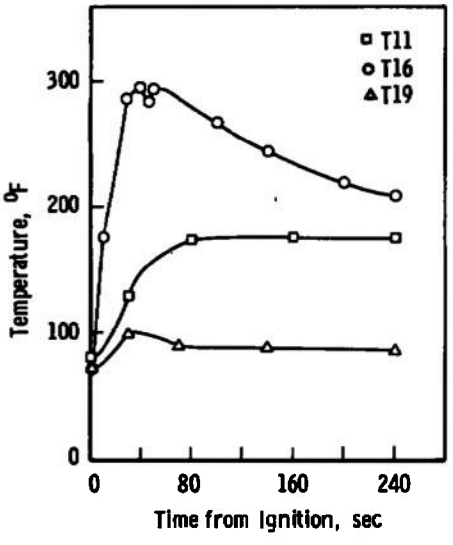

f. T11, T16, and T19

Fig. 11 Continued

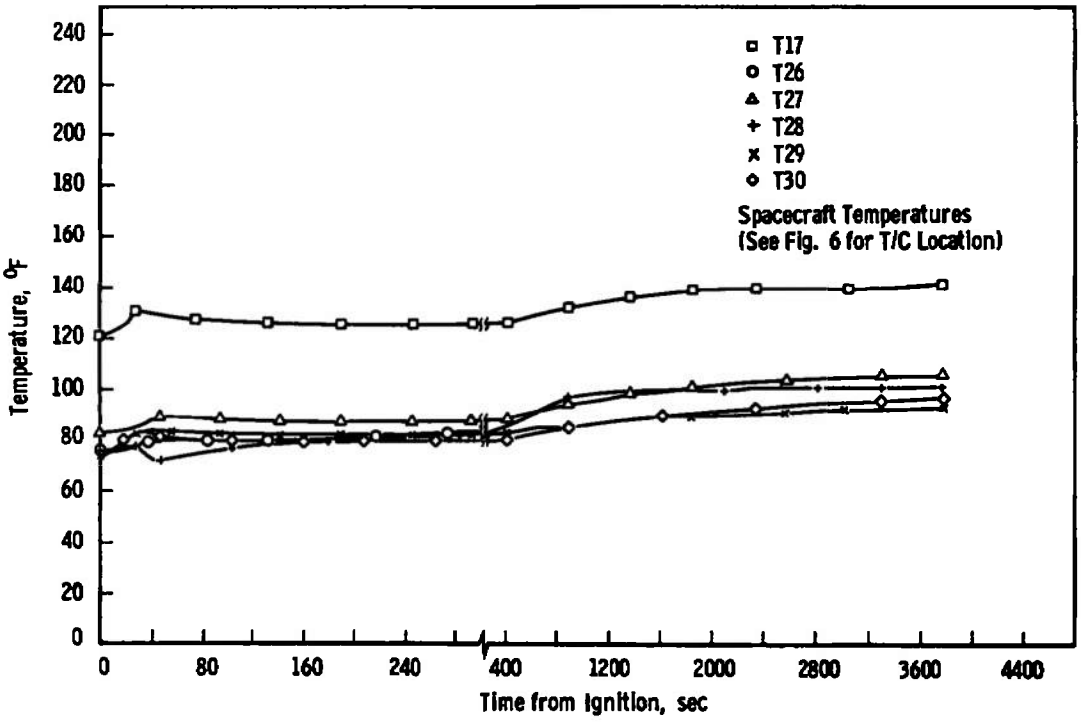

g. T17, T26, T27, T28, T29, and T30

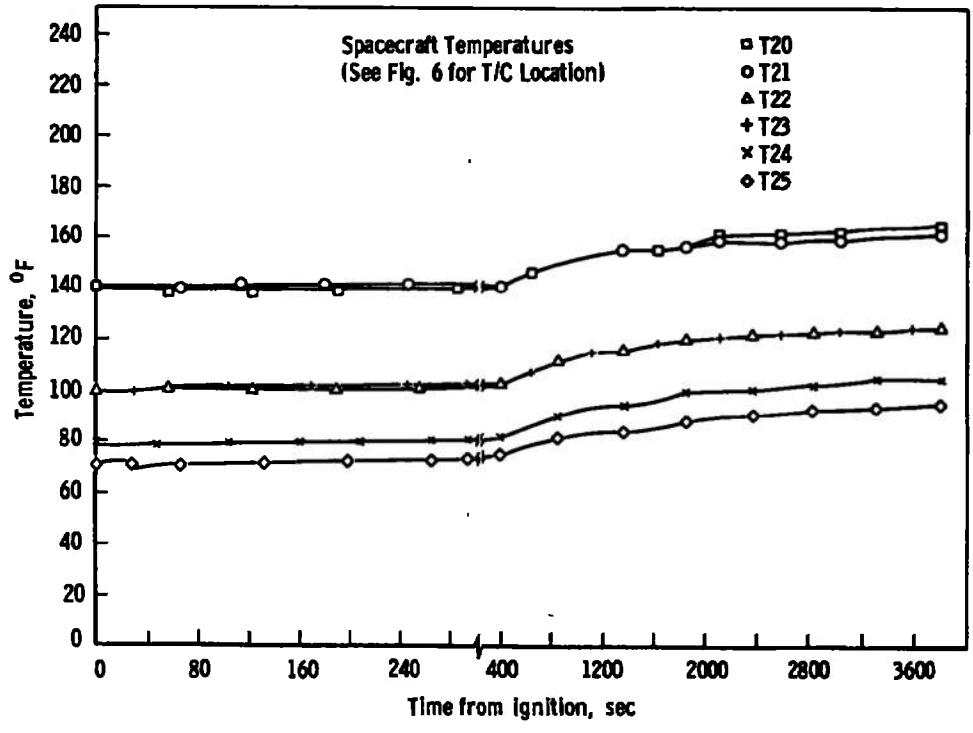

h. T20, T21, T22, T23, T24, and T25

Fig. 11 Continued

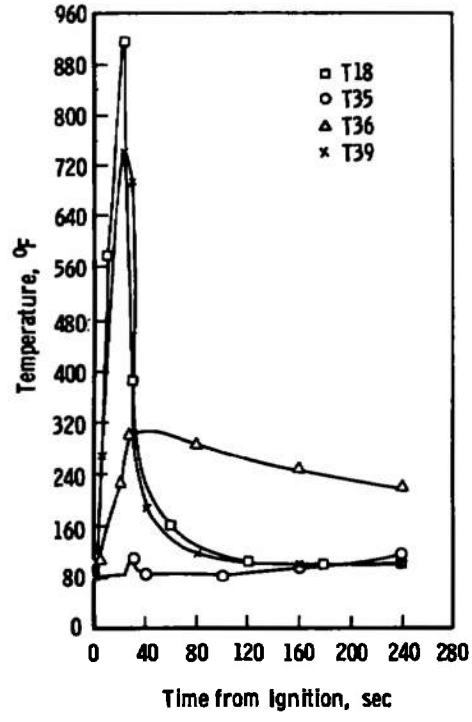

i. T18, T35, T36, and T39

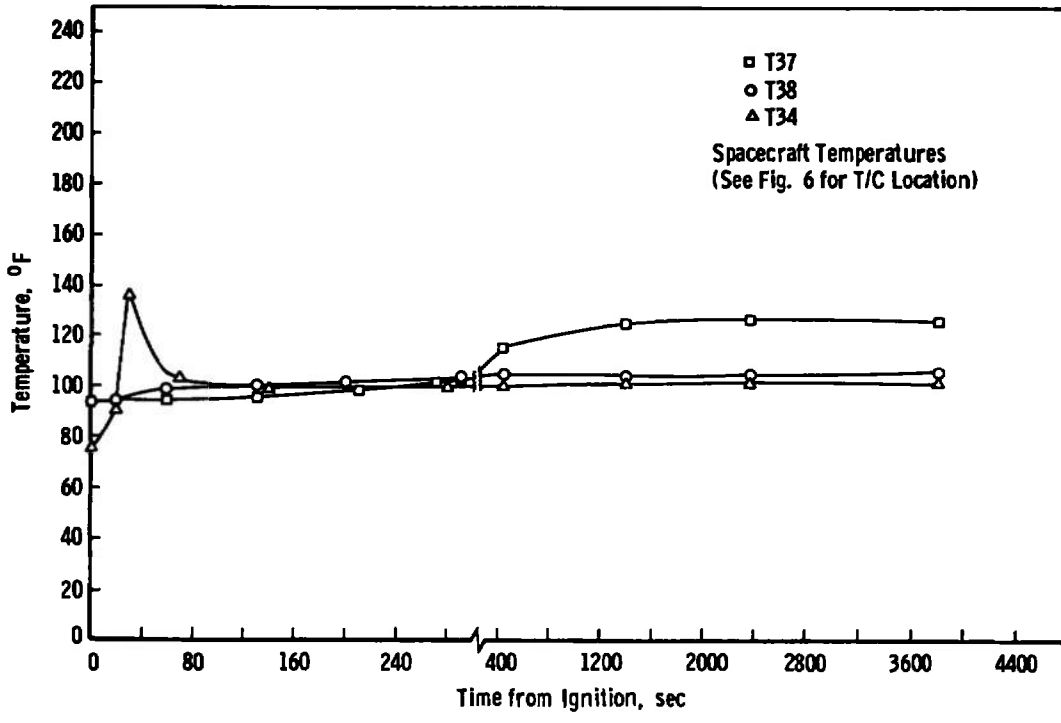

j. T34, T37, and T38

Fig. 11 Concluded

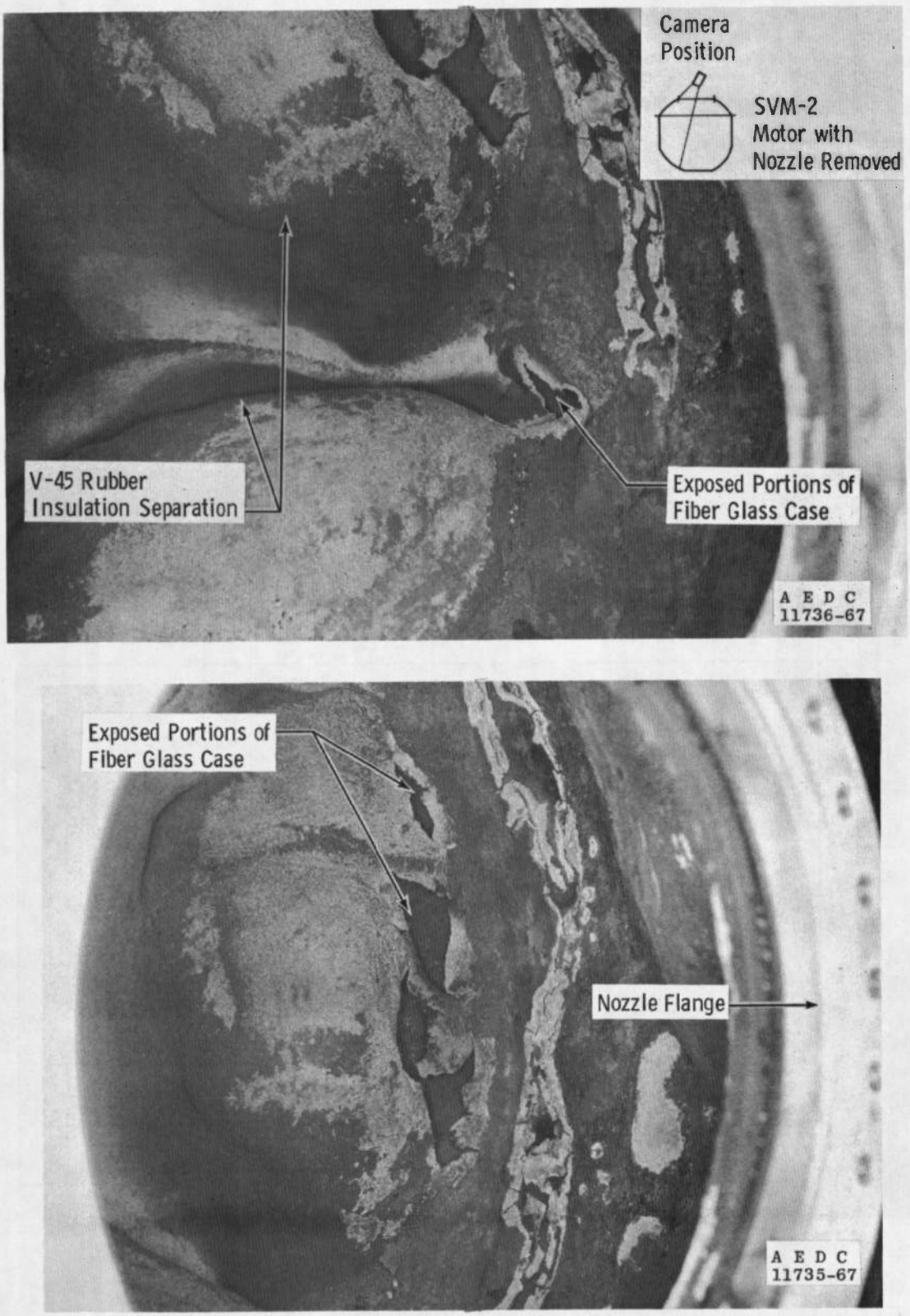

Fig. 12 Post-Fire Photographs of the SVM-2 Motor Interior

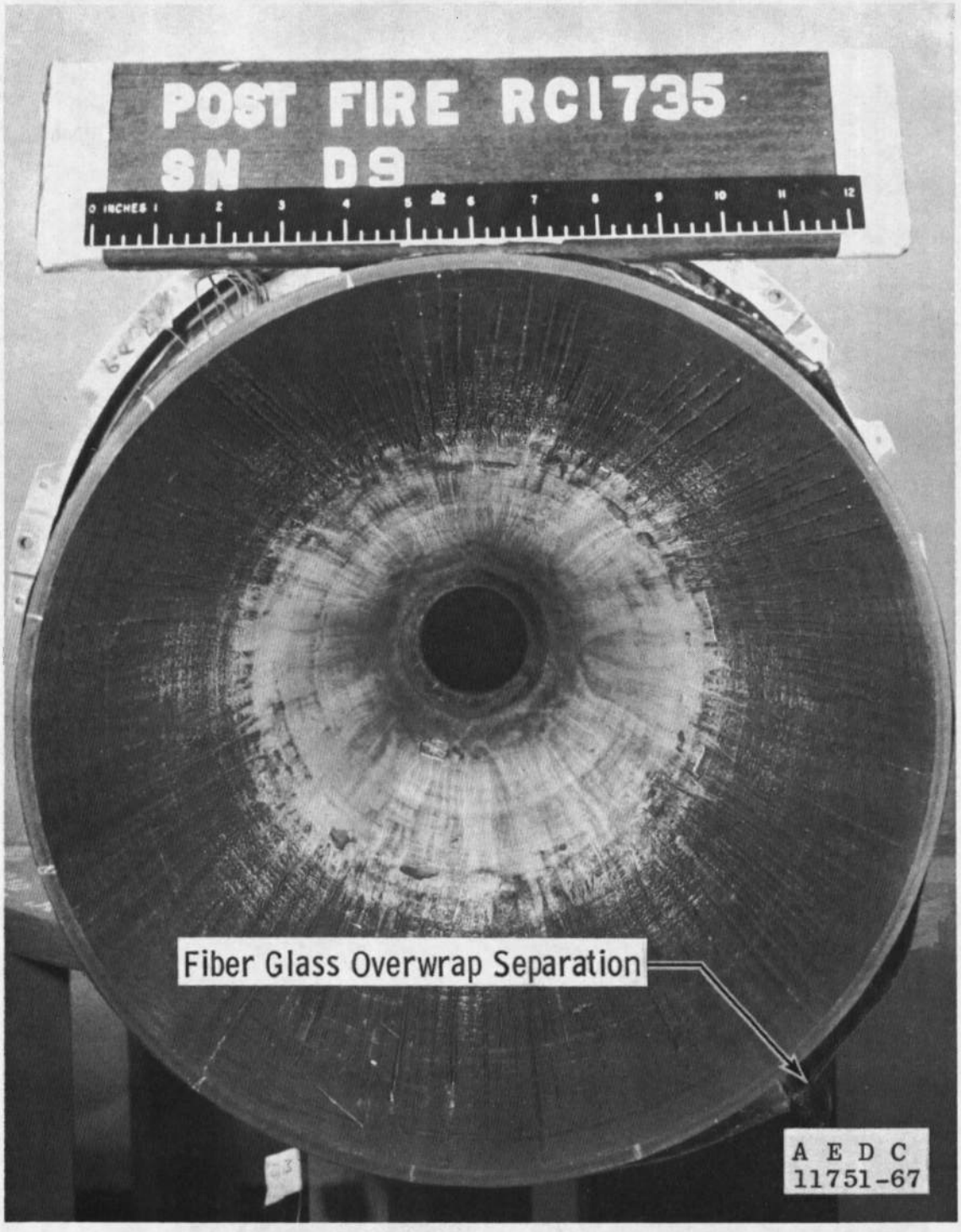

a. Interior of Exit Cone

Fig. 13 Post-Fire Photographs of the Nozzle Assembly

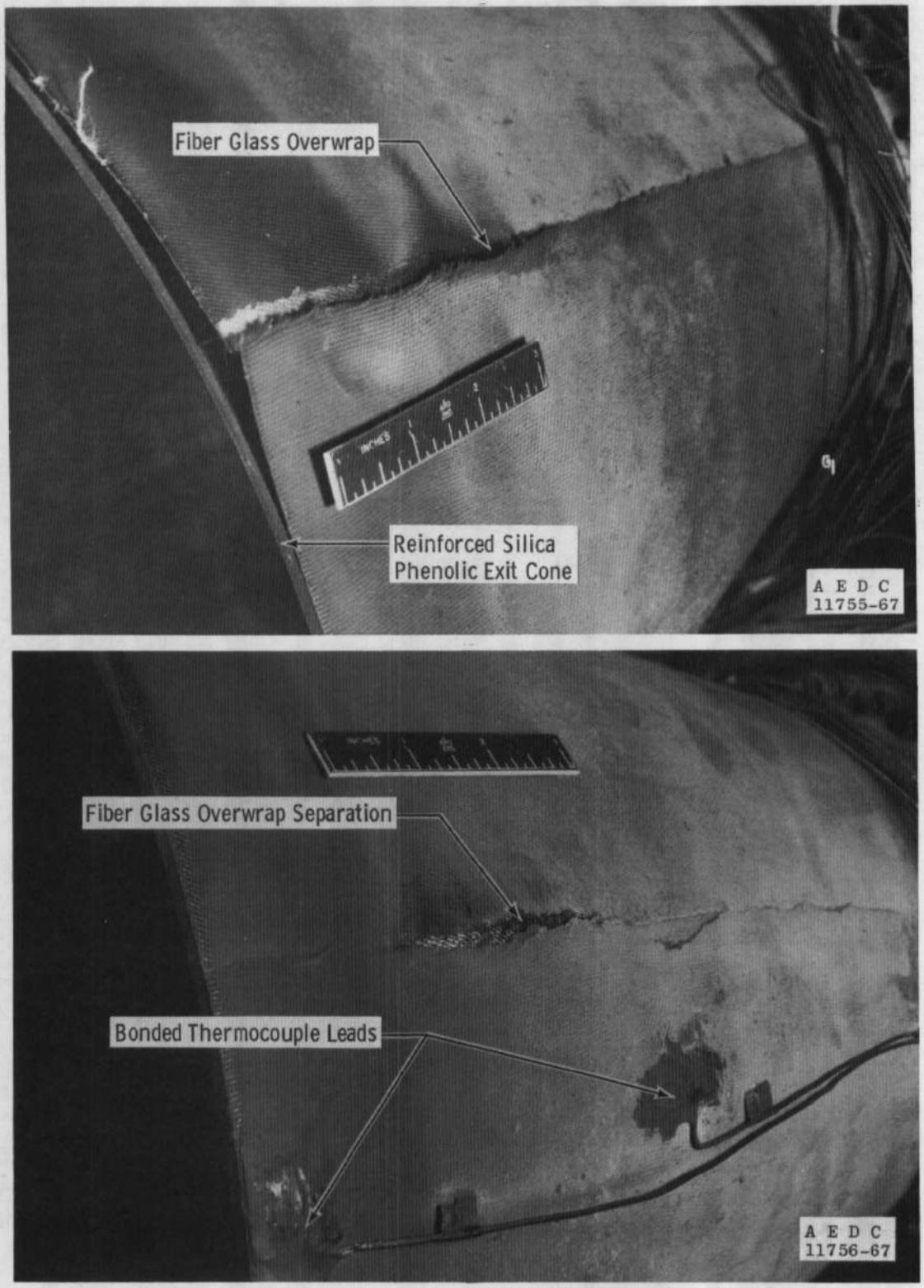

b. External Details (Separation of Fiber Gloss Overwrop)

Fig. 13 Continued

c. Nozzle Entrance Region

Fig. 13 Concluded

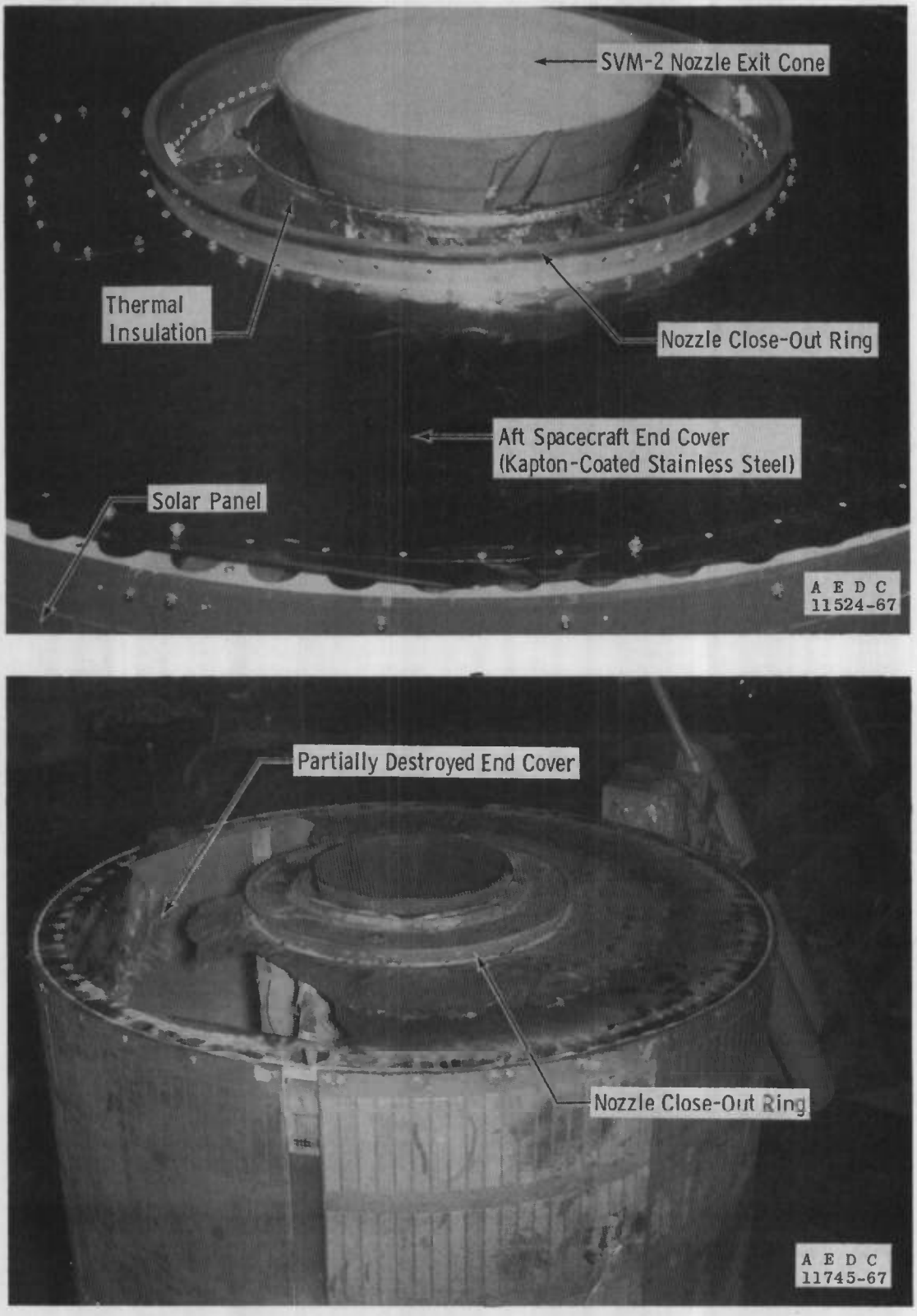

Fig. 14 Pre-Fire and Post-Fire Photographs of Spacecraft Aft Surface

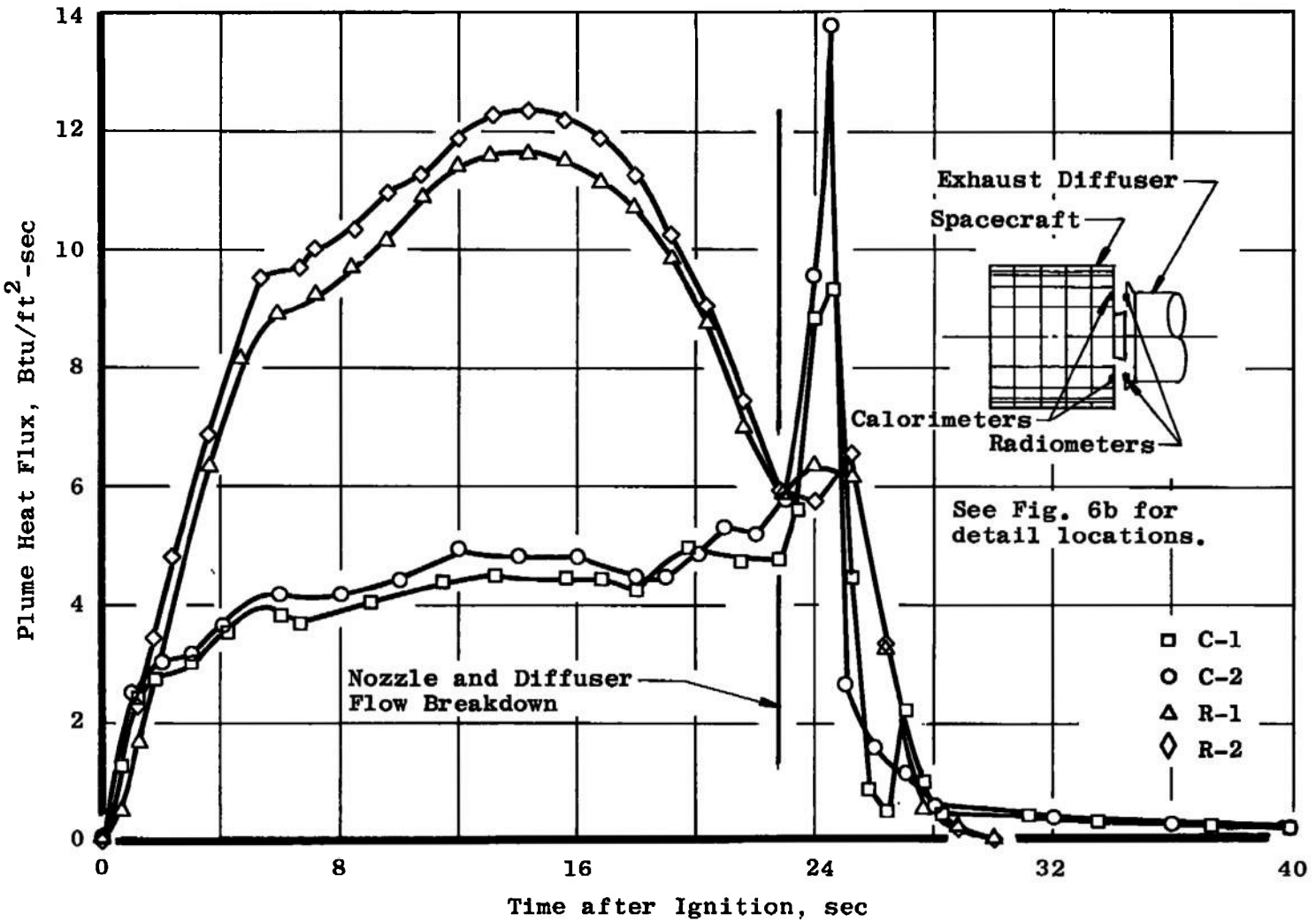

Fig. 15 Motor Exhaust Plume Radiation Heat Flux Variation with Time

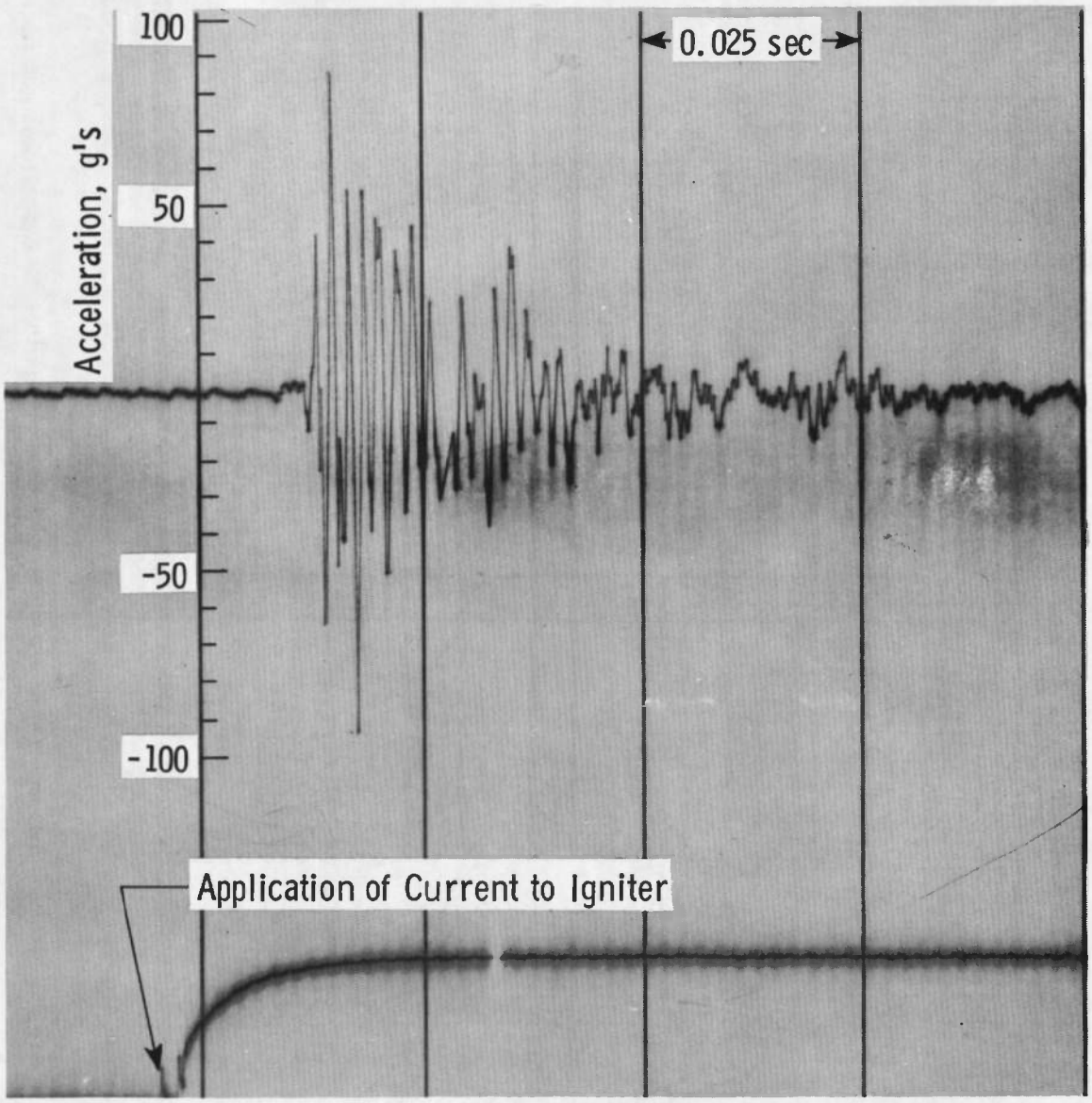

a. Accelerometer A5

Fig. 16 Vibration Data Obtained during the 0.1-sec Interval at Ignition

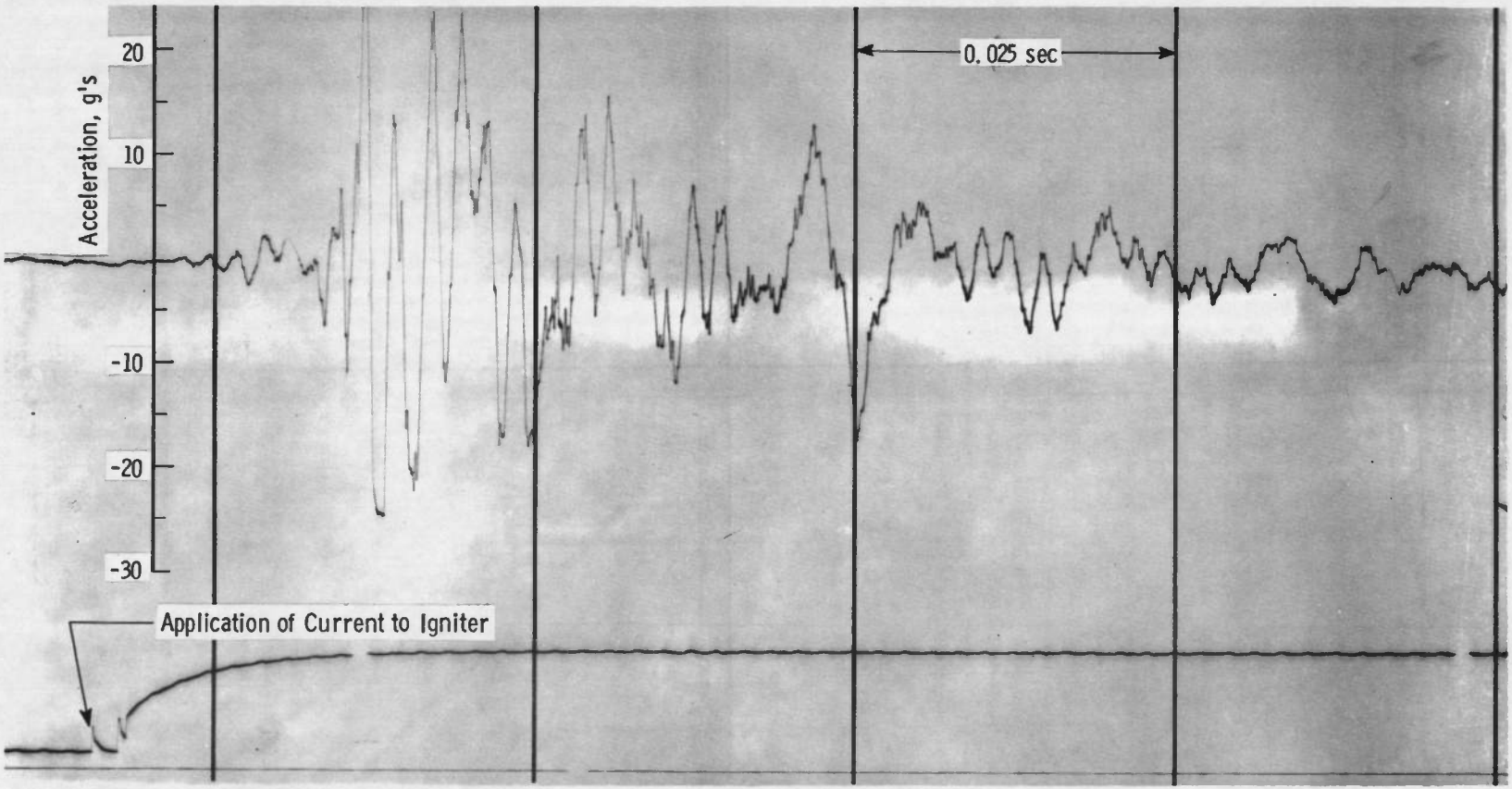

b. Accelerometer A3

Fig. 16 Continued

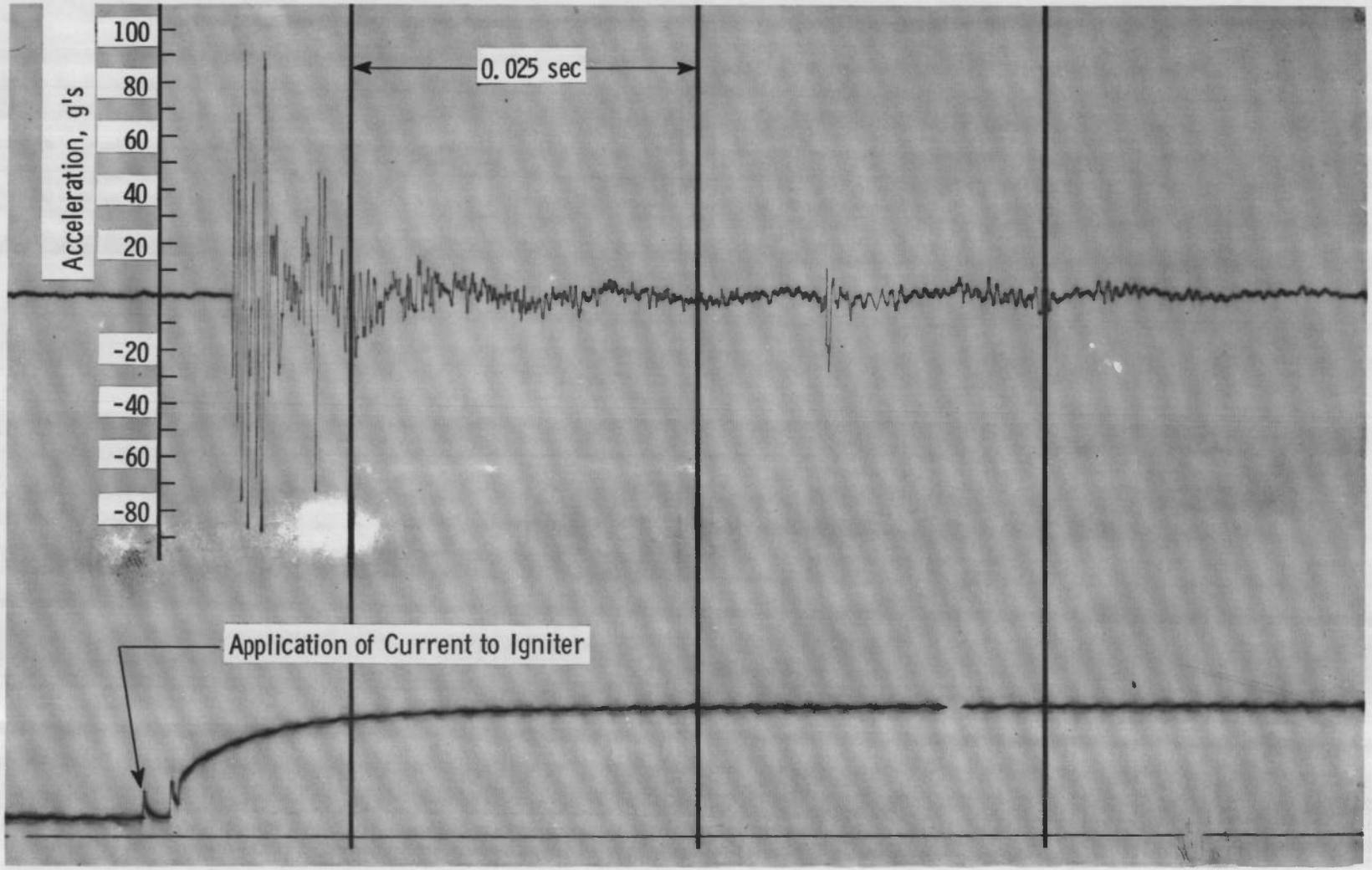

c. Accelerometer A1

Fig. 16 Continued

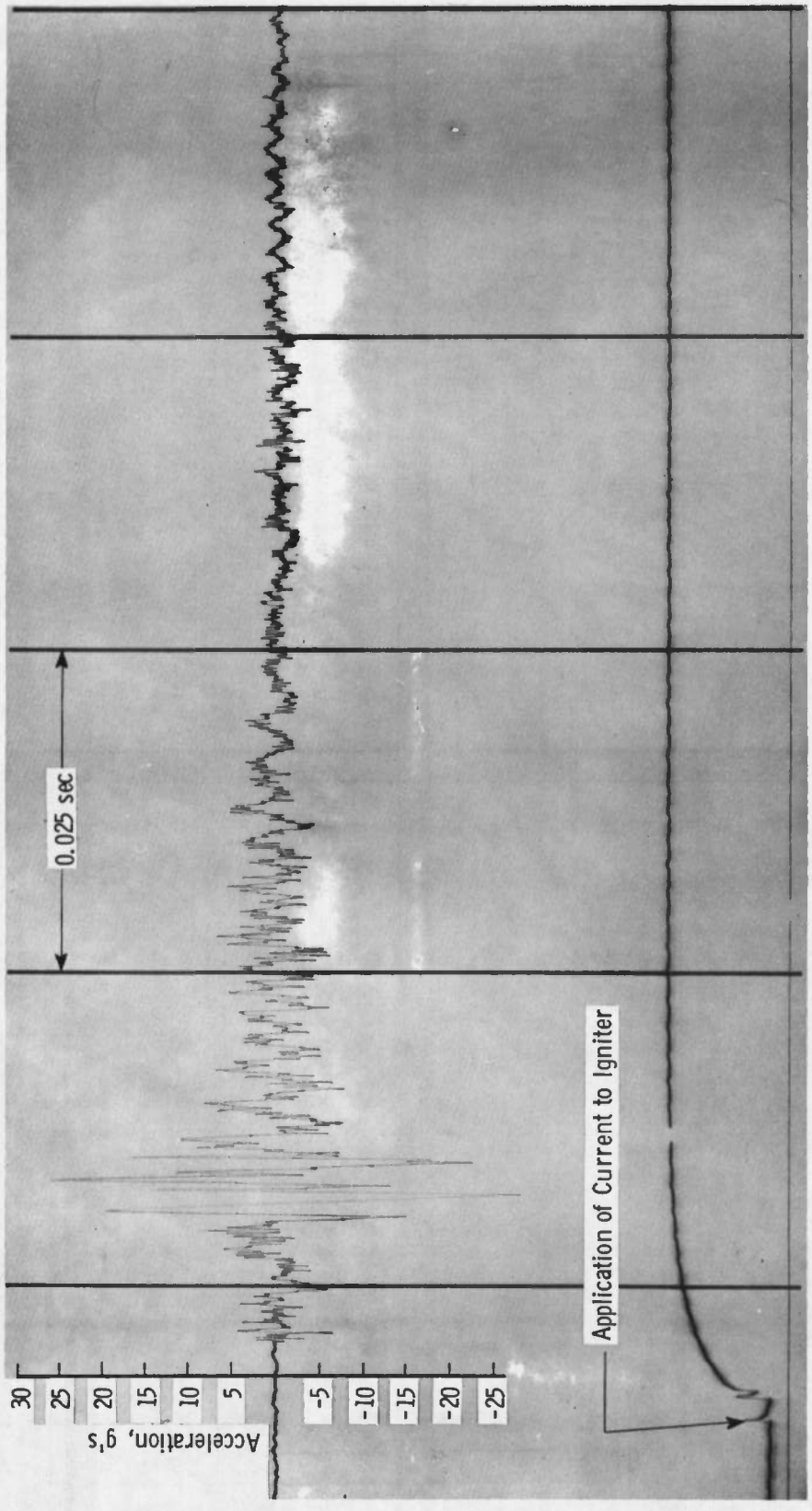

d. Accelerometer A4

Fig. 16 Concluded

TABLE I
STEADY-STATE MEASUREMENT UNCERTAINTY

Parameter	Estimated Measurement Uncertainty (2 Sigma)				Range of Measurement	Type of Measuring Device	Type of Recording Device	Method of System Calibration
	Steady-State at Operate Level, Percent of Reading	Integral, Percent of Reading	Over the Range of Measurement					
			Percent of Reading	Units of Measurement				
Axial Force, lb_f	±0.35	---	---	---	1640 to 5000 lb_f	Bonded Strain-Gage Force Transducer (2 Used)	Voltage-To-Frequency Converter onto Magnetic Tape	Deadweight
Total Impulse, lb_f-sec	---	±0.34	---	---	0 to 5000 lb_f			
Motor Chamber Pressure, psia	±0.28	---	---	---	155 to 455 psia	Bonded Strain-Gage Pressure Transducer (2 Used)		Resistance Shunt
Chamber Pressure Integral, psia-sec	---	±0.27	---	---	0 to 455 psia			
Low-Range Chamber Pressure, psia	---	---	±0.50	---	5 to 50 psia	(1 Used)		
Test Cell Pressure, psia	±1.17	---	---	---	0.062 to 0.41 psia	Unbonded Strain-Gage Pressure Transducer (3 Used)		
Test Cell Pressure Integral, psia-sec	---	±1.16	---	---	0 to 0.41 psia			
Event Time, msec	---	---	---	±5 msec	---	Synchronous Timing Line Generator	Photographically Recording Galvanometer Oscillograph	Compared to Frequency Standard
Spacecraft Temperature, °F	---	---	---	±5.5°F	0 to 800°F	Iron-Constantan Temperature Transducer	Sequential Sampling Millivolt-To-Digital Converter and Magnetic Tape Storage Data Acquisition System	Millivolt Source and NBS Temperature Tables
Motor Temperature, °F	---	---	---	±4.8°F	0 to 600°F	Chromel®-Alumel® Temperature Transducer		
Weight, lb_m	---	---	---	±0.031 lb_m	---	Beam Balance Scales	Visual Readout	Periodic Deadweight Calibration

TABLE II
SUMMARY OF MOTOR BALLISTIC PERFORMANCE

Motor S/N	D-9
Test Date (1967)	September 8
Ignition Altitude, ft	125,000
Pre-Fire Motor Temperature, °F	81
Average Altitude, ft	110,000
Ignition Lag Time(1), sec	0.007
Time from Ignition to Diffuser Flow Breakdown(2), t_{bd}, sec	22.70
Action Time(3), sec	25.40
Total Burn Time(4), sec	71.80
Measured Total Impulse (Average of Four Channels) (Ignition to t_{bd}), lb_f-sec	85,092
Maximum Deviation from Average, percent	0.072
Chamber Pressure Integral (Average of Two Channels) (Ignition to t_{bd}), psia-sec	7890.4
Maximum Deviation from Average, percent	0.059
Cell Pressure Integral (Average of Three Channels) (Ignition to t_{bd}), psia-sec	1.9869
Maximum Deviation from Average, percent	0.357
Average Axial Thrust (based on Action Time), lb_f	3472
Average Chamber Pressure (based on Action Time), psia	321
Chamber Pressure at which Nozzle and Diffuser Flow Breakdown Occurred, psia	146
Average Thrust Coefficient (based on 1 sec of data before diffuser flow breakdown), $\bar{c}_f$	1.837
Vacuum Total Impulse, lb_f-sec	88,719
Vacuum Specific Impulse, lb_f-sec/lb_m	
Based on Manufacturer's Stated Propellant Weight	284.35
Based on Expended Mass (AEDC)	281.05
Average Vacuum Thrust Coefficient (based on Action Time and Average Pre- and Post-Fire Throat Areas), C_F	1.846

(1)Interval from application of ignition voltage to time of increase in chamber pressure.

(2)Defined in Fig. 9.

(3)Time interval beginning when chamber pressure has risen to 10 percent of maximum (excluding ignition peak) and ending when chamber pressure has fallen to 10 percent of maximum at tailoff.

(4)The time interval between the first indication of chamber pressure at ignition and the time the ratio of chamber pressure to cell pressure decreases at 1.3 at tailoff.

TABLE III
SUMMARY OF MOTOR PHYSICAL DIMENSIONS

Test Date	September 8, 1967
Motor Serial Number	D-9
(AEDC) Weights (Motor)	
Pre-Fire Weight, lb_m	357.291
Post-Fire Weight, lb_m	41.620
Expended Mass, lb_m	315.671
Manufacturer's Stated Propellant Weight	
Propellant Grain	311.69
Igniter Grain	0.32
Total	312.01
Nozzle Throat Area, $in.^2$	
Pre-Fire	5.953
Post-Fire	5.766
Percent Change	-3.14
Average	5.860
Nozzle Exit Area, $in.^2$	
Pre-Fire	166.498
Post-Fire	165.492
Percent Change	-0.60
Average	166.001
Nozzle Area Ratio	
Pre-Fire	27.97
Post-Fire	28.70
Average	28.33

UNCLASSIFIED

Security Classification

DOCUMENT CONTROL DATA - R & D

(Security classification of title, body of abstract and indexing annotation must be entered when the overall report is classified)

1. ORIGINATING ACTIVITY *(Corporate author)*
Arnold Engineering Development Center
ARO, Inc., Operating Contractor
Arnold Air Force Station, Tennessee

2a. REPORT SECURITY CLASSIFICATION
UNCLASSIFIED

2b. GROUP
N/A

3. REPORT TITLE
TEST OF THE INTELSAT III COMMUNICATION SPACECRAFT AND APOGEE MOTOR UNDER THE COMBINED EFFECTS OF SIMULATED ALTITUDE AND ROTATIONAL SPIN

4. DESCRIPTIVE NOTES *(Type of report and inclusive dates)*
Final Report - September 8, 1967

This document has been approved for public release its distribution is unlimited. Per A. F. Letter Dated 4 April 73, Signed by William D. Cole

5. AUTHOR(S) *(First name, middle initial, last name)*
L. R. Bahor and R. M. Brooksbank, ARO, Inc.

6. REPORT DATE	7a. TOTAL NO. OF PAGES	7b. NO. OF REFS
December 1967	57	2

8a. CONTRACT OR GRANT NO.	9a. ORIGINATOR'S REPORT NUMBER(S)
AF 40(600)-1200	AEDC-TR-67-273
b. PROJECT NO. 9033	
c. Program Area 921E	9b. OTHER REPORT NO(S) *(Any other numbers that may be assigned this report)*
d.	N/A

10. DISTRIBUTION STATEMENT Subject to special export controls; transmittal to foreign governments or foreign nationals requires approval of National Aeronautics and Space Administration, Goddard Space Flight Center, Greenbelt, Md.

11. SUPPLEMENTARY NOTES	12. SPONSORING MILITARY ACTIVITY
Available in DDC.	National Aeronautics and Space Administration, Goddard Space Flight Center, Greenbelt, Md.

13. ABSTRACT

An Aerojet-General Corporation SVM-2 solid-propellant apogee rocket motor installed in an Engineering Model (EM-2) of the INTELSAT III communications spacecraft was fired while spinning at 100 rpm at a pressure altitude of 125,000 ft. The primary objective of the program was verification of vacuum performance of the apogee motor after being conditioned at 75 ± 5°F. Secondary objectives were to evaluate the thermal and mechanical interactions on the spacecraft as a result of the motor firing. Electrical heaters were utilized in the EM-2 to simulate the heat loads of the active electrical equipment contained in the actual spacecraft. Altitude ignition characteristics and ballistic performance are presented and discussed. Temperature-time histories of thermocouples placed at selected locations on the motor are presented. Spacecraft vibration data and motor exhaust plume heat flux data are also presented and discussed.

DD FORM 1 NOV 65 1473

UNCLASSIFIED

Security Classification

UNCLASSIFIED

Security Classification

14. KEY WORDS	LINK A		LINK B		LINK C	
	ROLE	WT	ROLE	WT	ROLE	WT
/ INTELSAT III						
spacecrafts, communications						
rocket motors						
solid propellants						
spin test						
altitude tests						
performance						

2. Missiles -- Intelsat III

3. Apogee motors -- Performance

3 50 R

" " "

2. [redacted] 16-3

UNCLASSIFIED

Security Classification